coatings

MDPI

Article

The Influence of the Q-SUN and UV-B Irradiation on the Antiviral Properties of the PP Films Covered with the Coatings Based on ZnO Nanoparticles and TiO_2

Małgorzata Mizielińska * and Artur Bartkowiak

Center of Bioimmobilisation and Innovative Packaging Materials, Faculty of Food Sciences and Fisheries, West Pomeranian University of Technology Szczecin, Janickiego 35, 71-270 Szczecin, Poland; artur.bartkowiak@zut.edu.pl

* Correspondence: malgorzata.mizielinska@zut.edu.pl; Tel.: +48-91-449-6132

Abstract: The purpose of this research was to analyze the antiviral activity of coatings based on ZnO nanoparticles and TiO_2. The goal was also to investigate the influence of accelerated UV-B and Q-SUN irradiation on their effectiveness. The results of the performed analysis demonstrated that only one of four coatings containing nanoparticles demonstrated high antiviral activity. Q-SUN irradiation had a positive influence on the antiviral properties of the other three coatings. After 24 h of accelerated irradiation, these coatings demonstrated moderate antiviral effectiveness, confirming that Q-SUN irradiation improved the properties of the active layers (by activating ZnO nanoparticles and TiO_2). Unfortunately, after 48 h of irradiation, the activity of the coatings decreased, confirming that the irradiation time should not be too long. Comparing the influence of the UV-B irradiation on the coating activity to the Q-SUN irradiation, it has to be mentioned that UV-B irradiation (24 h) also improved the antiviral properties of the three coatings, which were not active before irradiation. However, it decreased the activity of the coating that was active before UV aging. Unfortunately, none of those analyzed coatings were active after 48 h of UV-B irradiation, confirming that the irradiation time should be shorter.

Keywords: antiviral activity; phi6 phage; active coatings; UV-B irradiation; Q-SUN irradiation; TiO_2; ZnO nanoparticles

Citation: Mizielińska, M.; Bartkowiak, A. The Influence of the Q-SUN and UV-B Irradiation on the Antiviral Properties of the PP Films Covered with the Coatings Based on ZnO Nanoparticles and TiO_2. *Coatings* **2024**, *14*, 125. https://doi.org/10.3390/coatings14010125

Academic Editor: Klemen Bohinc

Received: 13 December 2023
Revised: 7 January 2024
Accepted: 15 January 2024
Published: 17 January 2024

1. Introduction

Severe Acute Respiratory Syndrome-Coronavirus-2 (SARS-CoV-2) is an agent that causes coronavirus disease (COVID-19). Despite the available treatments against SARS-CoV-2 and vaccination, there are still about 767 million cases of daily worldwide infections, including over 6.9 million deaths, due to the COVID-19 pandemic [1,2]. Additionally, RNA viruses, which have a high mutation rate, like SARS-CoV-2, increase the risk of multi-resistant variant development with more virulence characteristics [1]. This virus, which is highly communicable, is mainly transmitted though respiratory droplets and aerosols during human-to-human interactions [3] or indirectly through physical contact, usually via the hands after being deposited on surfaces, such as packaging [2]. The spread of virus particles has demonstrated the necessity to develop novel materials with antimicrobial properties to prevent the infection of current viruses and yet-unknown variants that could appear in the future [1–4]. Antiviral surface material treatments may influence virus particles through a reduction in their number or can directly avoid these hazards [4]. Consequently, the use of highly efficient, low-cost, environmentally friendly antiviral coatings on surfaces or as an external packaging material layer could be a reasonable solution to mitigate the transmission of viral diseases.

The antimicrobial properties of various metals nanoparticles, such as ZnO, TiO_2, copper and silver nanoparticles, have been extensively studied and documented [2,5–7].

Zinc oxide nanoparticles hold antimicrobial properties for Gram-negative and Gram-positive bacteria to spores highly resistant to high temperatures and pressure environments, yeasts, mold [6–10] and viruses [1,3]. Zinc oxide nanoparticles have been introduced into polymer matrices derived from petroleum, using conventional incorporation methods, such as melt mixing or solvent casting, as well as being added to polymer coating layers in the application of antimicrobial packaging or surfaces [6,7]. Zhou et al. [11] noted that negatively charged ZnO nanoparticles may simply trap the virus particles and inhibit their attachment to the host cells. When ZnO was co-cultured with viruses and cells, the cell survival rate increased by over 50%. Additionally, an external coating of packaging or a surface covered with an active coating should be active in storage/usage, meaning it has to be able to be sufficiently resistant against the irradiation of UV, be protected against UV light by the use of an additive or be activated by UV. This means that introducing active substances, such as ZnO nanoparticles that are resistant to UV aging in a coating carriers or adding an agent with shielding properties, may not only prevent the inactivation of the external coating/surface after UV aging but can even increase its antimicrobial activity [5–7]. It is worth mentioning that ZnO nanoparticles exhibit shielding properties [6,7]. Additionally, the activity of the zinc oxide nanoparticles and their shielding properties may depend on their structure/morphology. The nanoparticles can be observed as lens-like ZnO pyramidal crystals, which may grow in the form of diamonds, in which there is a hexagonal base and a conical tip. Those diamond-like ZnO structures were noted to give the nanomaterials extraordinary optical properties [12].

Photocatalytic nanoparticles such as titanium dioxide (TiO_2) may also be used for surface coatings or packaging external coating fabrication to limit the spread of bacterial cells and viruses particles from the most commonly touched surfaces or from packed-food products by a photo-inducible antimicrobial effect [13]. Mirzapoor et al. [13] found that titanium dioxide or titania (TiO_2)-covered surfaces minimized microbial adhesion via altering the surface free energy. Due to the optical band gap (3.2 eV), reactivity, stability, reusability, biocompatibility, durability, crystallinity, corrosion resistance, high surface area and, most importantly, low cost, TiO_2 was found to be the best candidate as an antimicrobial agent, which could attack microorganisms with reactive oxygen species (ROS) [14,15]. TiO_2 nanoparticles have offered great potential for the deactivation of phage MS2, phage f2, HIV, norovirus, etc. It is also worth mentioning that UV-active TiO_2 was found to increase virus inactivation owing to its antimicrobial activity towards genetically similar SARS-CoV-2 and HCoV [15,16].

Comparing ZnO and TiO_2 nanoparticles as photoactive metal oxides, it was shown that both ZnO and TiO_2 as excellent semiconductors were effective against hepatitis C, polio, H1N1 influenza, herpes, SARS-CoV, SARS-CoV-2, etc. [15,17–19]. Many authors investigated metal doping as an effective method to extend the spectral response of TiO_2 to a visible region, as well as to decrease the electron–hole recombination rate [14,20–24]. It was reported by the authors [14,22] that TiO_2 doped with 10% $CuCl_2$ resulted in a complete inhibition of 100% *Escherichia coli* growth compared to TiO_2. In a great deal of recent research, the light absorption extension of TiO_2 into the visible region has been investigated through the doping of TiO_2 with ZnO nanoparticles [13]. The authors suggest that zinc oxide nanoparticles with a direct wide band gap of 3.3 eV may be used in an antiviral coating to improve TiO_2 photocatalyst efficiency [13,25,26]. Liu et al. [9] obtained micro-arc oxidation (MAO) coatings containing Zn, which were fabricated on Ti6Al4V alloys using EDTA-ZnNa2 electrolytes (Zn-doped coatings on Ti6Al4V alloys). The authors clearly showed that the reactive oxygen species (ROS) level of MAO samples was significantly higher than that of the uncovered Ti6Al4V. Zn-doped coatings caused the strongest oxidative stress on Gram-positive bacteria compared to uncoated alloys (due to the relatively high released Zn^{2+} concentration). The results from previously carried out work by the authors [6] demonstrated that active coatings that contained geraniol, carvacrol and nano ZnO were found to be effective against both Gram-positive and Gram-negative bacteria, confirming a synergistic effect between zinc oxide nanoparticles and geraniol or carvacrol. Against a phi 6 phage, the coatings only offered modest activity. However, the

synergistic effect between ZnO nanoparticles and TiO_2, which were introduced into the coating carrier, such as a solvent gloss varnish to create an active layer, is not confirmed. Additionally, previous investigations demonstrated that UV irradiation did not decrease the antibacterial activity of the coatings containing ZnO nanoparticles into a coating carrier [27] or into the polymer matrix after UV aging [5]. However, the effect of Q-SUN or UV-B irradiation on the antiviral properties of the coatings containing ZnO nanoparticles was not analyzed in any previous work. These findings have led to the implication that coatings containing ZnO nanoparticles and TiO_2 could be active towards viruses, such as SARS-CoV-2, and that there is a synergistic effect between these two active agents. After Prussin II, A.J. et al. [28] proposed that the Phi6 bacteriophage could be used as a substitute/surrogate for the SARS-CoV-2 together with influenza viruses, and based on previous research [6], the phi 6 phage was selected to determine the antiviral properties of the coatings.

In summary, the purpose of the research was to examine the coatings' (based on a solvent varnish contained in the ZnO nanoparticles and TiO_2) antiviral activity. The goal was also to investigate the influence of accelerated UV-B and Q-SUN irradiation on the effectiveness of these active layers.

2. Materials and Methods

2.1. Materials

Both the bacterial strain and phage phi6 to be used in this experiment were acquired from a collection offered by the Leibniz Institute DSMZ (Deutsche Sammlung von Mikroorganismen und Zellkulturen, Braunschwelg, Germany). The microorganism utilized in this research was *Pseudomonas syringae* van Hall 1902 DSM 21482. The phi 6 phage (DSM-21518) was used as a SARS-CoV2 substitute. Polypropylene films (A4, 20 µm) were supplied by MarDruk (Andrychów, Poland). The coating carrier, which was used in these experiments, was a solvent gloss varnish 70 GU279686 (Hubergroup, Warsaw, Poland) and, in addition, zinc oxide AA 44899 (~70 nm) powder (Thermo Fisher GmbH, Kandel, Germany) and TiO_2 (Grupa Azoty, Police, Poland), which were used as antiviral compounds. The 99.8% ethanol (EU-ROCHEM BGD Sp. z o.o. Tarnów, Poland) was used as a solvent. Luria-Bertani (LB) broth and Agar-Agar (Merck, Darmstadt, Germany) were taken to determine the antiviral activity of any coatings. All media were prepared in accordance with the Merck protocol (all of the media had to be weighed according to manufacturer instructions and were then suspended in 1000 mL of distilled water and autoclaved at 121 °C for 15 min).

2.2. Coating Preparation

Each of the coating dispersions was prepared according to the scheme (Figure 1). Briefly, 0.031 g of ZnO nanoparticles was added to 50 mL of 99.8% ethanol. Initially, a one-hour mixing process of dispersion took place using a magnetic stirrer (Ika, Warsaw, Poland) at 450 rpm. Next, sonication took place for 30 min (parameters: cycle: 0.5; 20% amplitude). A ZnO nanoparticle dispersion was added to 50 g of the solvent gloss varnish (coating carrier) and mixed for 10 min at 750 rpm (Zn coating). As next step, 0.031 g of ZnO nanoparticles and 0.031 g of TiO_2 (1:1) were introduced into 50 mL of 99.8% ethanol. A magnetic stirrer at 450 rpm mixed the dispersion for an hour. Next, the dispersion underwent sonication for 30 min (parameters: described above). A dispersion of ZnO and TiO_2 was added to 50 g of the coating carrier and stirred for 10 min at 750 rpm (ZnT1 coating). Consequently, step dispersions containing (a) 0.031 g of ZnO nanoparticles and 0.0405 g of TiO_2 (1:1.5) and (b) 0.031 g of ZnO nanoparticles and 0.062 g of TiO_2 (1:2) were introduced into 50 mL of 99.8% ethanol (separately). These dispersions were then stirred and sonicated as described above. Finally, the dispersions were mixed with varnish and stirred for 10 min at 750 rpm (ZnT2 and ZnT3 coatings). Table 1 contains the content of the coating dispersions.

A Unicoater 409 (Erichsen, Hemer, Germany) was used to coat the polypropylene (PP) films at 25 °C with a 40 µm diameter roller. The coatings were dried for a period of 10 min at 50 °C. The control samples (PP) were PP films that had not been covered.

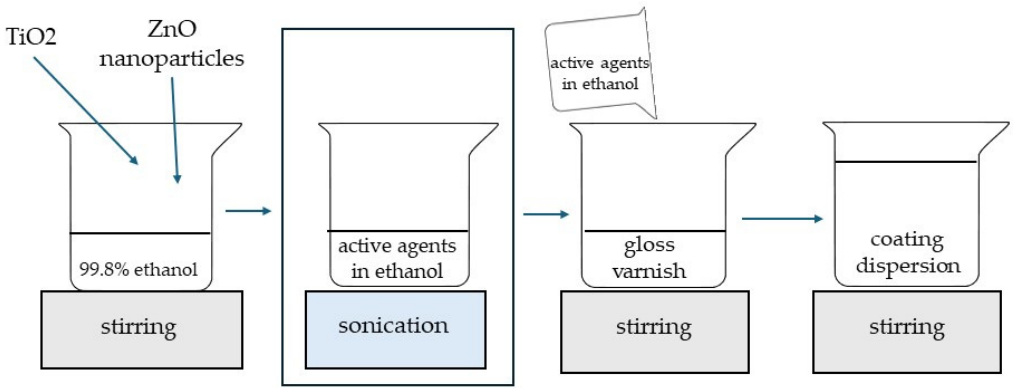

Figure 1. Coating dispersion preparation scheme.

Table 1. The content of the coating dispersions.

Dispersion Ingredients	Active Coatings			
	Zn	**ZnT1**	**ZnT2**	**ZnT3**
ZnO [g]	0.031	0.031	0.031	0.031
TiO_2 [g]	0	0.031	0.0405	0.062
99.8% ethanol [mL]	50	50	50	50
solvent gloss varnish 70 GU279686 [mL]	50	50	50	50

The samples of PP film and coated PP films (before and after irradiation) were then sliced into squares (3 cm × 3 cm) for an analysis of antiviral activity.

2.3. UV Irradiation

The PP films, which were non-coated, as well as the PP films covered with active layers were all cut into rectangles (23.5 × 7.0 cm and 26.0 × 2.5 cm), respectively. The aforementioned samples were introduced into (1) a weathering tester that utilized UV-B acceleration with 1.55 W/m^2 (Q-LAB DEUTSCHLAND GMBH, Saarbrucken, Germany) and irradiated for 24 h at 60 °C; (2) a Q-SUN accelerated Xenon Test Chamber with 1.5 W/m^2 (Model Xe-2, Q-LAB DEUTSCHLAND GMBH, Saarbrucken, Germany) and irradiated for 24 h at 47 °C (black panel) and at 39 °C (chamber air) with an RH of 40%.

2.4. Antiviral Activity Analysis

Initially, the particles of phi6 phage were refined according to Bhetwal et al. [29]. Later, the pure bacteriophage lysate was prepared according to Bonilla et al. [30]. The antiviral properties of the active coatings that contained nanoparticles were compared to non-covered films, with this taking place according to a modified ISO 22196-2011 standard [31]. As a final stage, an amplification of the phage occurred through the use of a method suggested by Skaradzińska et al. [32]. Antiviral analysis was carried out for the sample films/films covered with coatings before their irradiation and after Q-SUN and UV-B irradiation.

To analyze the real-time growth rate of the *P. syringae* (phi 6 phage host) with phages, after incubation with the antiviral coating, bacteriophage lysate was incubated with the non-covered PP films (control) and with samples that were coated with active layers (with each active coating individually) according to ISO 22196-2011 [31]. The LB broth was added to 5 BioSan bioreactors (BS-010160-A04, BioSan, Riga, Latvia). *P. syringae* overnight culture was later added to 10 mL of LB broth, and this was incubated at 28° when OD = 0.2 (optical density). Five phi 6 bacteriophage lysates were amplified in their own respective host bacteria (1 lysate—after its incubation with the non-covered film (control sample), 4 lysates—after their incubation (separately) with the active coatings containing ZnO nanoparticles and TiO_2). Next, 10 µL of phage lysate (MOI = 1) was added to host cultures (OD = 0.2) and incubated at 28° (until OD for the control sample decreased). Five simultaneous tests were carried out, meaning that it was possible to

analyze 4 active coatings within one experiment. An analysis of the *P. syringae* growth rate in real time was performed for films/coatings before their irradiation and after Q-SUN and UV-B irradiation.

2.5. SEM Analysis

2.5.1. SEM Analysis of the Active Coatings

The PP films and PP films covered with Zn, ZnT1, ZnT2 and ZnT3 active layers were analyzed using a scanning electron microscope (SEM). As a first step, the samples before and after their Q-SUN and UV-B irradiation (for 24 h and 48 h, respectively) were placed on pin stubs with carbon tape and covered with a layer of gold in a sputter coater at 24 °C (Quorum Technologies Q150R S, Laughton, East Sussex, UK). SEM tests were performed using a Vega 3 LMU microscope (Tescan, Brno-Kohoutovice, Czech Republic). The goal of this analysis was to visually confirm that the PP films had been thoroughly and homogeneously covered with the active layers. The SEM was carried out through the use of a tungsten filament with an accelerating voltage of 10 kV.

2.5.2. *P. syringae* Counts Visualization

SEM analysis was carried out to visualize *P. syringae* counts at the same time as lysis profile experiments. *P. syringae* and phage phi6 after its incubation with the selected, non-irradiated active coating (ZnT3: coating which was active toward phi 6 phage) were selected for this assay to verify that the incubation of the phage lysate active layer influenced phage activity, and these phage particles did not influence the growth of the host cells. *P. syringae* with phage phi6 after its incubation with the non-coated PP film (control sample had no influence on the phage activity) and lysate after its incubation with the ZnT1 coating (coating which was not active against phi 6 phage) were used as lysis control. Lysis profile tests were carried out on a smaller scale in Eppendorf tubes in a 1 mL final volume. After a period of 6 h incubation at 28 °C, the *P. syringae* and phage phi6 samples were placed in room-temperature conditions (24 °C). Grids of carbon-coated copper (400 mesh) were then placed in the liquid samples fully immersed, and the bacterial cells were given 30 min to adhere. Later, the prepared grids were removed from Eppendorf tubes, placed on petri dishes, and sterile paper sheet was used to remove the excess liquid and they were then left to dry. For a period of 18 h at 4 °C, the samples were then fixed (2% glutaraldehyde in a 0.1 M sodium cacodylate (NaCac, pH 7.4)). Later, the samples were washed in 0.1 M sodium cacodylate and dehydrated at 1 h intervals in serial concentrations of ice-cold (−20 °C) methanol (10%, 20%, 40%, 60%, 80% and 100%). The samples were left on pin stubs where a coating of thin gold layer was added in a sputter coater at room temperature (Quorum Technologies Q150R S, Laughton, East Sussex, UK). Further on, a microscopic analysis was performed using a Vega 3 LMU (Tescan) scanning electron microscope (SEM). An analysis was performed at room temperature with a tungsten filament, and an accelerating voltage of 20 kV was used to capture SEM images for the analyzed samples. All specimens were viewed from above.

2.6. FT-IR

Fourier-transform infrared (FT-IR) spectrum of the non-coated and coated PP film (before and after UV-B and Q-SUN) irradiation was measured using FT-IR spectroscopy (Perkin Elmer Spectrophotometer, Spectrum 100), operated at a resolution of 4 cm^{-1} and with eight scans. The non-coated and coated PP film samples were cut into squares (3 × 3 cm) and placed directly in the ray-exposing stage. The spectrum was recorded at a wavelength of 650–4000 cm^{-1}.

2.7. Statistical Analysis

When carrying out an analysis of variance (one-way ANOVA), statistical significance was noted, of considerably different values, where $p < 0.05$. The analyses were carried out by using GraphPad Prism 8 (GraphPad Software, San Diego, CA, USA).

3. Results

3.1. Antiviral Analysis

The results clearly demonstrated that a reduction in the bacteriophage titer was not seen in the case of the coating containing ZnO nanoparticles (Zn) than when placed side by side with the control sample (non-covered polypropylene PP film) (Figure 2). Figure 3 clearly shows an OD fall after 8 h of phage cultivation with the host for both samples of PP film and the alternative PP film covered with Zn coating, confirming that the Φ 6 particles were active. It should be mentioned that the PP film and the alternative PP film with a coating of Zn were incubated for 24 h with the phage particles. An OD fall confirmed that the particles were still active. Similar results were obtained for the host culture incubated with the phages after their incubation with the ZnT1 and ZnT2 coatings (separately) (Figure 3). Additionally, a reduction in the phi 6 phage particle number after their incubation with the ZnT1 or ZnT2 layer (compared to the control sample) was not noted. It seems clear that the differences between phage particle numbers were found to be insignificant, confirmed by statistical analysis. However, an OD fall was observed after 6.5 h (for a ZnT2 layer) and after 8.5 h (for a ZnT1 coating) of *P. syringae* incubation with the phage particles. The addition of phages should take place when the OD is about 0.2. The OD of the host was slightly lower than 0.2 when bacteriophage particles were added after their incubation with a ZnT2 coating, and this led to a fall in the OD after 6.5 h (not after 8 h). To summarize, the results confirmed that the incubation of the phages with the Zn, ZnT1 or ZnT2 coatings did not deactivate the phages nor reduce their number. It can be assumed that the Zn, ZnT1 and ZnT2 coatings had no antiviral activity. Contradictory results were noted in the case of the ZnT3 coating. As can be seen in Figure 3, an OD fall was not noted, even after phage cultivation up to 9.5 h with the host (when the OD for the control sample began to decrease after 7 h). The lack of OD fall in the host meant that the Φ 6 particles were not active. An analysis of the bacteriophage titer later confirmed these results. Figure 2 clearly shows that there was no reduction in bacteriophage particle number (compared to the PP film), but complete inactivation was observed. A 24 h phage incubation with the ZnT3 coating was seen to deactivate the phages completely. This might suggest that the ZnT3 coating demonstrated high antiviral activity, which resulted in a complete elimination of the active phage particles.

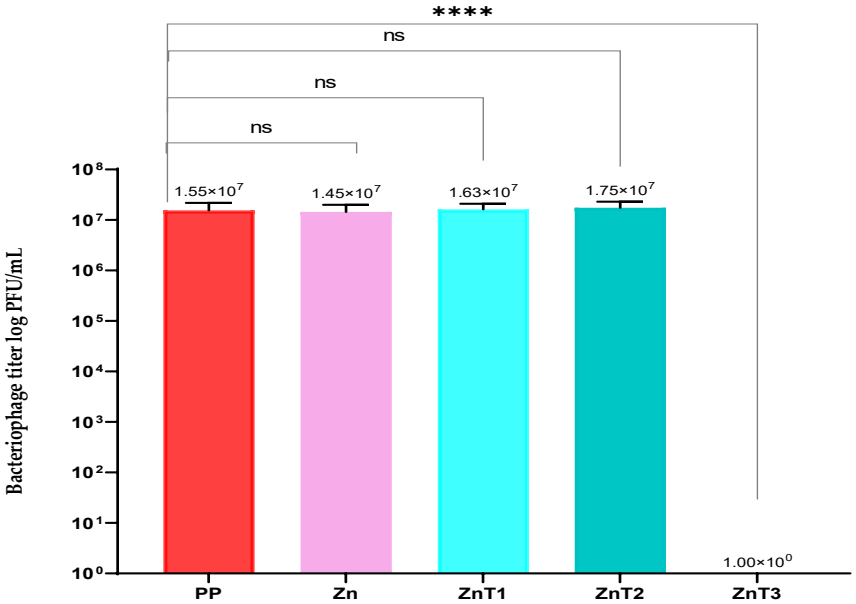

Figure 2. The influence of coatings on bacteriophage titer. PP—non-covered PP films; Zn—coating containing ZnO nanoparticles; ZnT1—coating containing ZnO nanoparticles and TiO_2 (in the ratio: 1:1); ZnT2—coating containing ZnO nanoparticles and TiO_2 (in the ratio: 1:1.5); ZnT3—coating containing ZnO nanoparticles and TiO_2 (in the ratio: 1:2) coatings; one-way ANOVA: ns—not significant, ****—$p < -0.0001$.

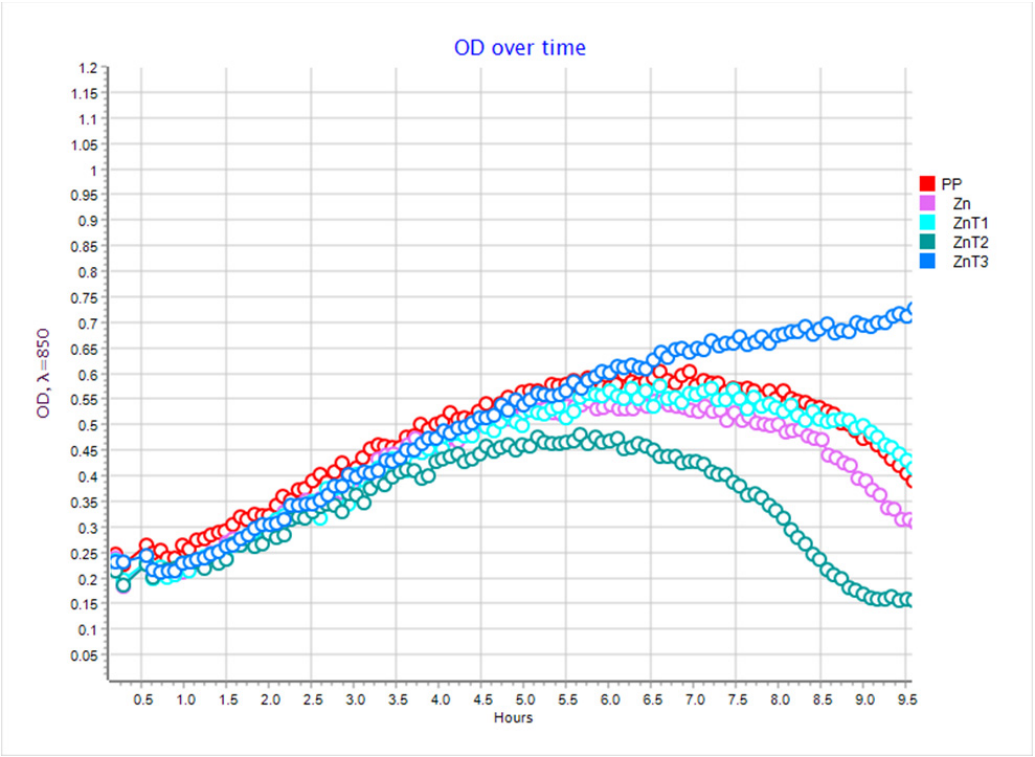

Figure 3. OD over time for *P. syringe* after 9.5 h of incubation. Incubation with phi 6 phages after their incubation with the PP films and with the Zn (coating containing ZnO nanoparticles), ZnT1 (coating containing ZnO nanoparticles and TiO_2 in the ratio: 1:1), ZnT2 (coating containing ZnO nanoparticles and TiO_2 in the ratio: 1:1.5), and ZnT3 (coating containing ZnO nanoparticles and TiO_2 in the ratio: 1:2) coatings; addition of phages when OD—0.2; amount of phage MOI—1.

An analysis with regard to the influence of the Q-SUN accelerated irradiation (24 h) on the antiviral activity of the coatings containing ZnO nanoparticles and TiO_2 as active agents demonstrated that in the case of the Zn, ZnT1 and ZnT2 coatings (Figure 4), there was a greater than 3 log reduction in the bacteriophages titer, compared to the non-coated PP film (the differences in the phage particles were significant according to statistical analysis). After 6 h of host incubation with phages, with the Zn, ZnT1 and ZnT2 coatings after irradiation for 24 h, the phages reduced the number of bacteria, leading to a slight fall in OD (Figure 5a). After 3 h, a decrease in the number of bacterial cells was observed for the phages, which were incubated for 24 h with the PP film. It can be assumed that the Zn, ZnT1 and ZnT2 coatings demonstrated moderate antiviral activity, resulting from the lack of any complete elimination of the active phage particles. Analyzing the effect of Q-SUN irradiation (for a 48 h) on the antiviral effectiveness of the active coatings indicated that in the case of the Zn, ZnT1 and ZnT2 coatings (Figure 4), a 2 log reduction (Zn coating) and lower than 1 log reduction (ZnT1 and ZnT2) in the phi 6 phage titer occurred (than when compared to the PP film). It was clear that after more than 6 h of incubation of the host with phages, incubated with the Zn, ZnT1 and ZnT2 coatings after their irradiation for 48 h, these phages decreased the number of the *P. syringae* cells, contributing to a fall in OD (Figure 5b). After 5 h, there was a clear degradation in the amount of host cells for phages that were incubated for 48 h with PP film. It can be concluded that the Zn layer had weak activity against phi 6 particles. It may be assumed that ZnT1 and ZnT2 coatings demonstrated even weaker antiviral activity than the Zn layer, which resulted from a lower reduction in the active phage particles. Contrary results were observed for the ZnT3 coating, which was irradiated for 24 h with the Q-SUN accelerated irradiation. As emphasized in Figure 5a, a fall in OD was not seen, even after 6 h of phage cultivation with the host (OD for the control sample decreased after 3.5 h). Additionally, Figure 2 clearly shows that there

was no reduction in the phi 6 phage particle number seen (compared to the irradiated PP film), but their complete inactivation occurred. The findings confirmed that phage incubation with an irradiated ZnT3 coating completely inactivated the phages. It can be assumed that 24 h irradiation of the samples using the Q-SUN chamber did not influence the effectiveness of the ZnT3 layer. This coating demonstrated high antiviral activity, resulting from a complete elimination of the active phage particles. Lower activity towards phi 6 phage was observed for the ZnT3 coating that was irradiated for 48 h. The incubation of phage lysate with this layer did not deactivate the particles completely but significantly decreased their number. A higher than 5 log reduction in the number of phage particles was noted for these samples (Figure 4). In addition, the OD fall was observed after 7 h of bacteriophage cultivation with the host. It can be assumed that after 48 h of irradiation, the ZnT3 coating was still active against the phi 6 phage, but its activity was insignificantly lower than the antiviral activity of the ZnT3 coating that was irradiated for 24 h.

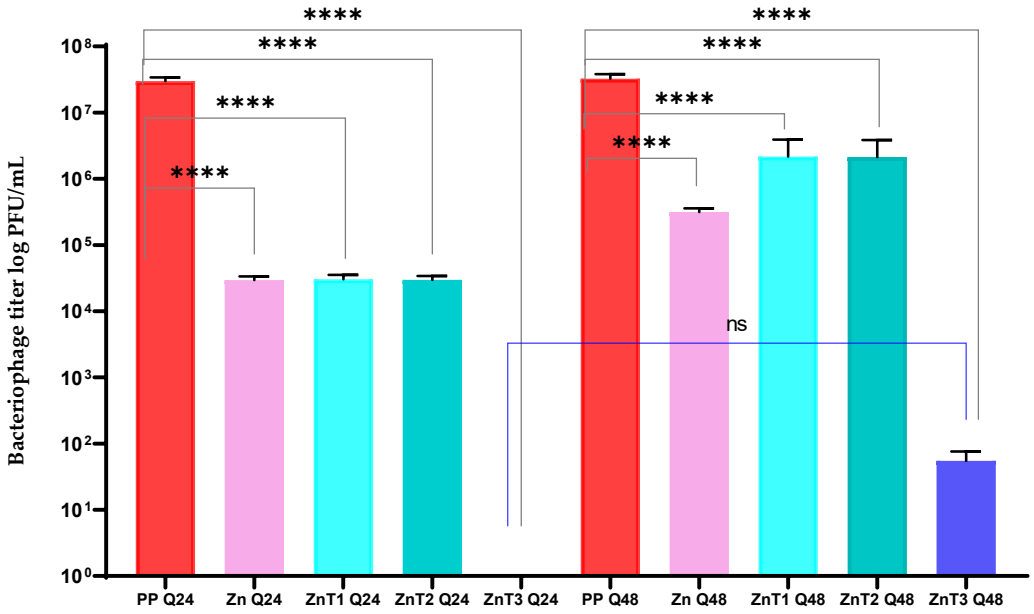

Figure 4. The influence of coatings that were irradiated 24 h and 48 h with the Q-SUN irradiation on bacteriophage titer. PP—non-covered PP films; Zn—coating containing ZnO nanoparticles; ZnT1—coating containing ZnO nanoparticles and TiO_2 (in the ratio: 1:1); ZnT2—coating containing ZnO nanoparticles and TiO_2 (in the ratio: 1:1.5); ZnT3—coating containing ZnO nanoparticles and TiO_2 (in the ratio: 1:2) coatings; one-way ANOVA: ns—not significant, ****—$p < -0.0001$.

An analysis of the influence of the UV-B irradiation (24 h) on the antiviral activity of the coatings containing nano ZnO and TiO_2 as active compounds confirmed that the 24 h irradiation increased the antimicrobial properties of the analyzed coatings. The results of this study clearly show (Figure 6) that phage incubation with irradiated coatings, Zn, ZnT2 and ZnT3, led to a significant reduction in the titer of bacteriophage (3 log) (according to a statistical analysis). Comparing the reduction in phage titer caused by active layers Zn, ZnT2 and ZnT3 and a reduction caused by irradiated ZnT1 coating (1 log reduction in the phage number), a noticeable increase in the antiviral activity of these coatings was observed. Analyzing the OD of the host cultivated with the phages over time (after incubation with UV-B irradiated PP film) demonstrated that after 4.5 h, a lowering OD was seen (Figure 7a). Almost identical results were found in the case of the irradiated ZnT1 coating, but the OD fall was observed after 5.5 h, which meant that phages lowered the number of host cells. A delayed bacteriolytic activity in the phages was seen in the case of both coatings, clearly showing that coating ZnT1 was only moderately active against the aforementioned phages. An analysis made in the case of

the OD of the *P. syringae*, cultivated with phages over time (after their incubation with UV-B irradiated Zn, ZnT2 and ZnT3), indicated that after 6 h, a fall in OD was not noted (Figure 7a). It could be said that Zn, ZnT2 and ZnT3 coatings exhibited moderate antiviral activity as a result of the reduction in the phage titer (3 log, Figure 6) but was devoid of complete elimination of any active phage particles. Analysis on the influence of the longer UV-B irradiation (48 h) on the antiviral effectiveness of coatings Zn, ZnT1, ZnT2 and Zn3 demonstrated that 48 h irradiation did not increase the Zn, ZnT1 and ZnT2 coating activity and even decreased the ZnT3 coating's antiviral properties when compared to the non-irradiated coating (Figure 7b). Additionally, 48 h of UV-B irradiation decreased the activity of all analyzed coatings compared to the samples irradiated for 24 h. The results of this study showed that an incubation of phages with irradiated Zn, ZnT1, ZnT2 and ZnT3 layers did not reduce the titer of the phages, even marginally (Figure 6). In the case of Zn, ZnT1, ZnT2 and ZnT3 coatings, after 5.5 h host cultivation with phages (after incubation with the irradiated coatings), a fall in OD was noted. It seems clear that phages that were still active reduced the amount of *P. syringae* (Figure 7b). This conclusively shows that UV-B-irradiated coatings Zn, ZnT1, ZnT2 and ZnT3 were not active against the phages.

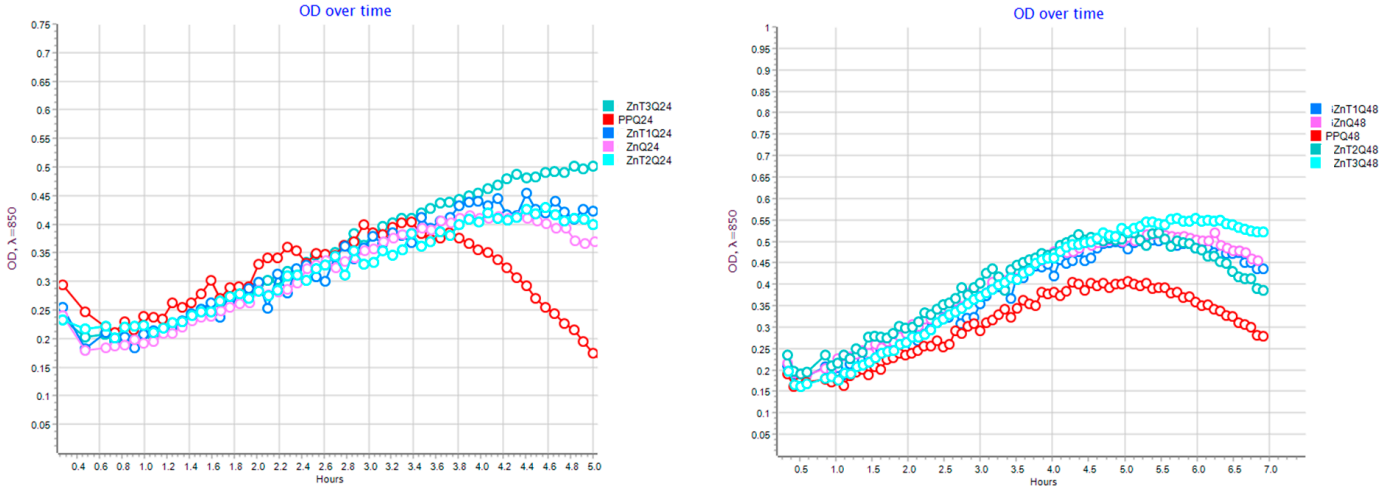

(**a**) (**b**)

Figure 5. (**a**). OD over time for *P. syringe* after 5.0 h of incubation. Incubation with phi 6 phages after their incubation with the irradiated PP films and with the Zn (coating containing ZnO nanoparticles, irradiated 24 h with the Q-SUN irradiation), ZnT1 (coating containing ZnO nanoparticles and TiO_2 in the ratio: 1:1; irradiated 24 h with the Q-SUN irradiation), ZnT2 (coating containing ZnO nanoparticles and TiO_2 in the ratio: 1:1.5; irradiated 24 h with the Q-SUN irradiation), and ZnT3 (coating containing ZnO nanoparticles and TiO_2 in the ratio: 1:2; irradiated 24 h with the Q-SUN irradiation) coatings; addition of phages when OD—0.2; amount of phage MOI—1. (**b**). OD over time for *P. syringe* after 7.0 h of incubation. Incubation with phi 6 phages after their incubation with the irradiated PP films and with the Zn (coating containing ZnO nanoparticles, irradiated 48 h with the Q-SUN irradiation), ZnT1 (coating containing ZnO nanoparticles and TiO_2 in the ratio: 1:1; irradiated 48 h with the Q-SUN irradiation), ZnT2 (coating containing ZnO nanoparticles and TiO_2 in the ratio: 1:1.5; irradiated 48 h with the Q-SUN irradiation), and ZnT3 (coating containing ZnO nanoparticles and TiO_2 in the ratio: 1:2; irradiated 48 h with the Q-SUN irradiation) coatings; addition of phages when OD—0.2; amount of phage MOI—1.

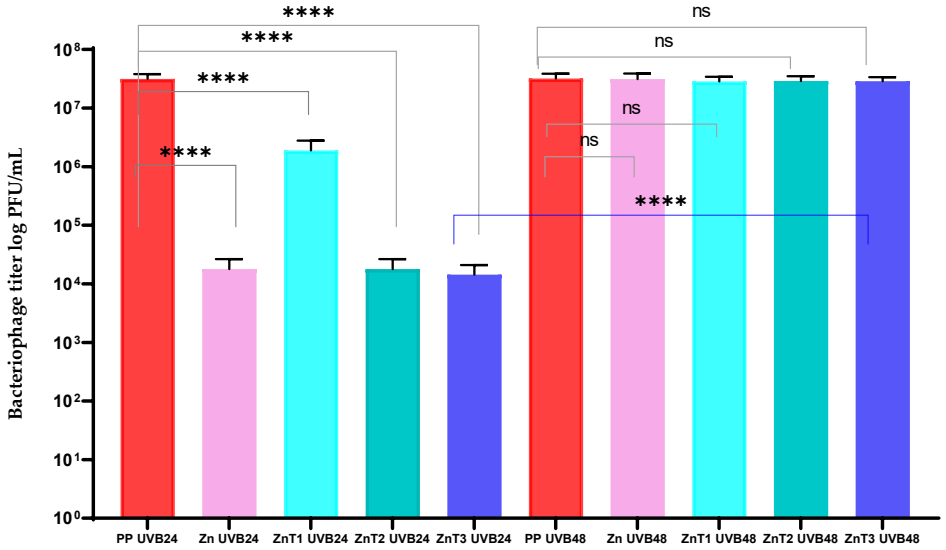

Figure 6. The influence of coatings that were irradiated 24 h and 48 h with the UV-B irradiation on bacteriophage titer. PP—non-covered PP films; Zn—coating containing ZnO nanoparticles; ZnT1—coating containing ZnO nanoparticles and TiO_2 (in the ratio: 1:1); ZnT2—coating containing ZnO nanoparticles and TiO_2 (in the ratio: 1:1.5); ZnT3—coating containing ZnO nanoparticles and TiO_2 (in the ratio: 1:2) coatings; one-way ANOVA: ns—not significant, ****—$p < -0.0001$.

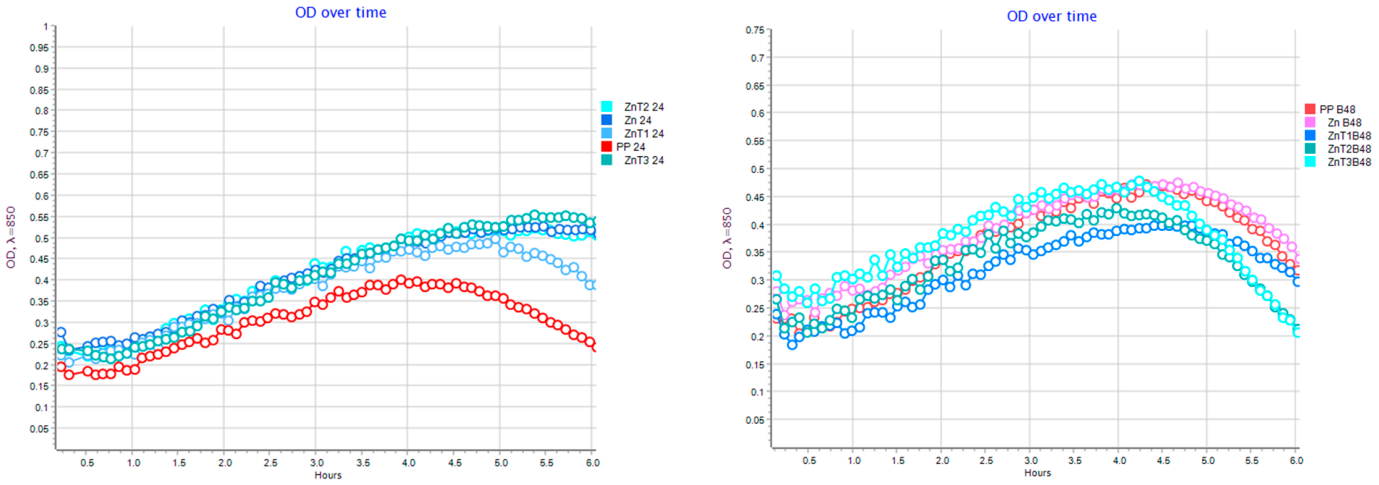

(**a**) (**b**)

Figure 7. (**a**). OD over time for *P. syringe* after 6.0 h of incubation. Incubation with phi 6 phages after their incubation with the irradiated PP films and with the Zn (coating containing ZnO nanoparticles, irradiated 24 h with the UV-B irradiation), ZnT1 (coating containing ZnO nanoparticles and TiO_2 in the ratio: 1:1; irradiated 24 h with the UV-B irradiation), ZnT2 (coating containing ZnO nanoparticles and TiO_2 in the ratio: 1:1.5; irradiated 24 h with the UV-B irradiation), and ZnT3 (coating containing ZnO nanoparticles and TiO_2 in the ratio: 1:2; irradiated 24 h with the UV-B irradiation) coatings; addition of phages when OD—0.2; amount of phage MOI—1. (**b**). OD over time for *P. syringe* after 6.0 h of incubation. Incubation with phi 6 phages after their incubation with the irradiated PP films and with the Zn (coating containing ZnO nanoparticles, irradiated 48 h with the UV-B irradiation), ZnT1 (coating containing ZnO nanoparticles and TiO_2 in the ratio: 1:1; irradiated 48 h with the UV-B irradiation), ZnT2 (coating containing ZnO nanoparticles and TiO_2 in the ratio: 1:1.5; irradiated 48 h with the UV-B irradiation), and ZnT3 (coating containing ZnO nanoparticles and TiO_2 in the ratio: 1:2; irradiated 48 h with the UV-B irradiation) coatings; addition of phages when OD—0.2; amount of phage MOI—1.

3.2. SEM Analysis

3.2.1. SEM Analysis of the Coatings

The SEM analysis was carried out for the samples before their irradiation and after 24 h and 48 h or accelerated irradiation with the magnification of 100×, 200×, 500×, 1000×. Figures 8–12 show selected micrographs (with magnification of 500×) after 48 h of sample irradiation because the differences between the samples irradiated for 24 h and 48 h were not observed.

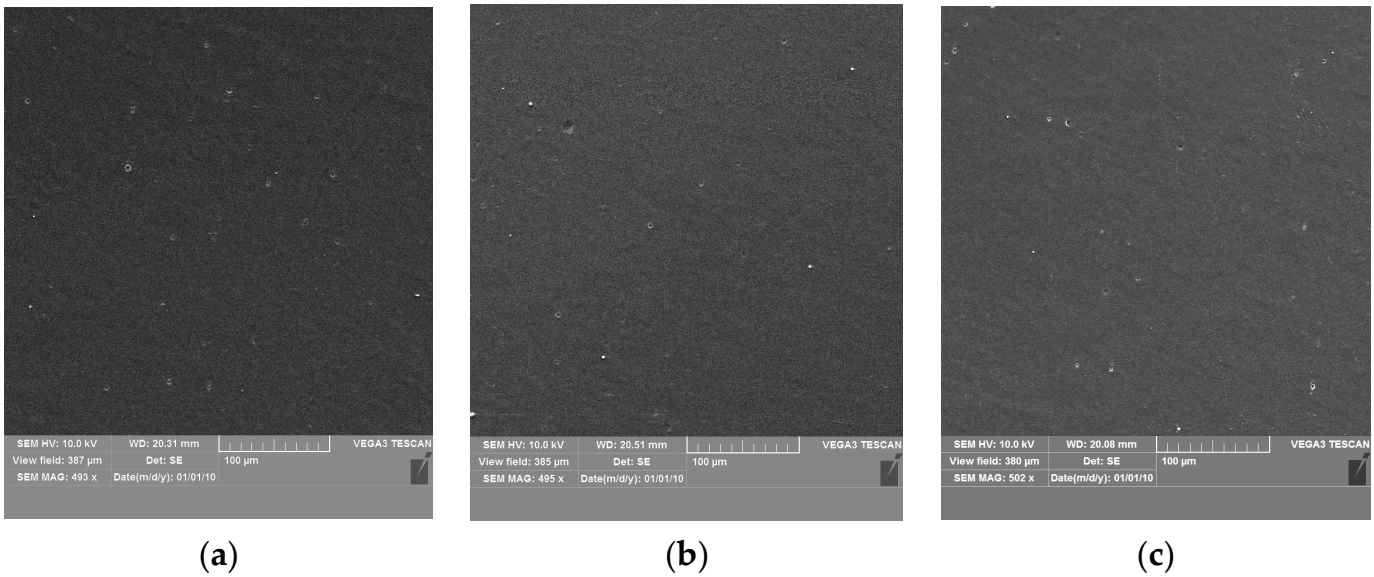

(**a**) (**b**) (**c**)

Figure 8. (**a**) PP films before irradiation; (**b**) PP films after 48 h of Q-SUN irradiation; (**c**) PP films after 48 h of UV-B irradiation.

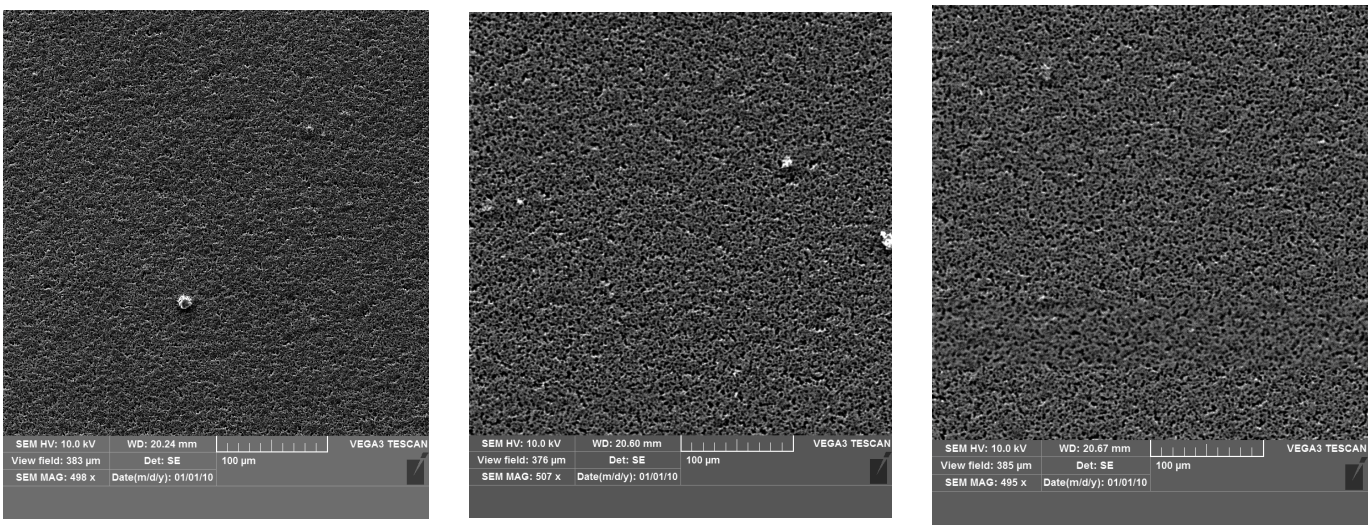

(**a**) (**b**) (**c**)

Figure 9. (**a**) PP films covered with Zn coating before irradiation; (**b**) PP films covered with Zn coating after 48 h of Q-SUN irradiation; (**c**) PP films covered with Zn coating after 48 h of UV-B irradiation.

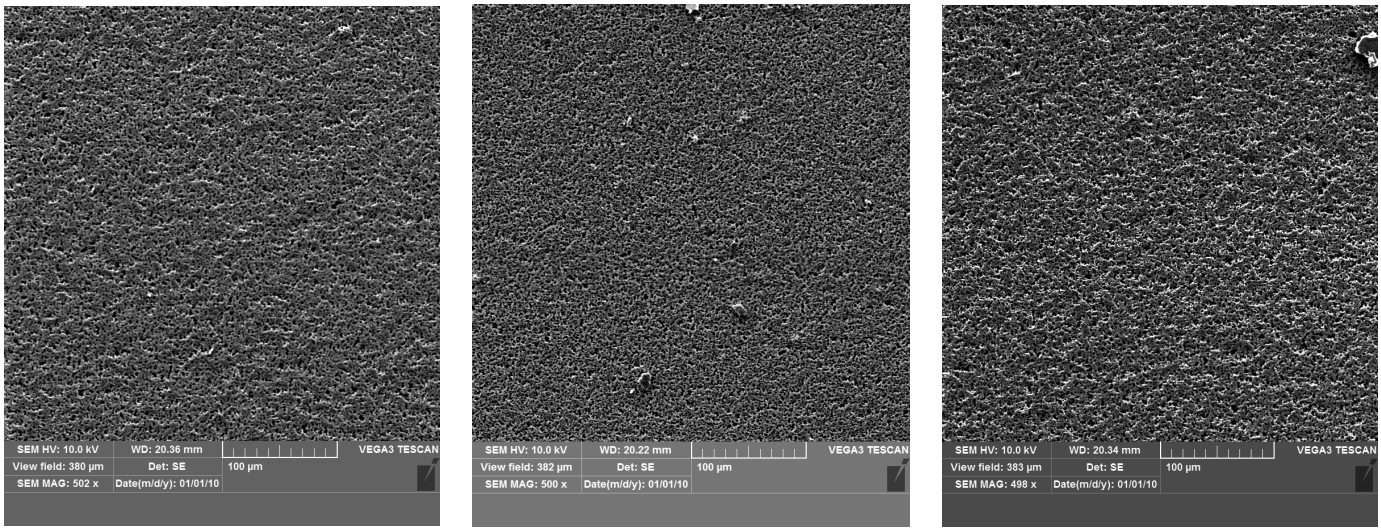

(**a**) (**b**) (**c**)

Figure 10. (**a**) PP films covered with ZnT1 coating before irradiation; (**b**) PP films covered with ZnT1 coating after 48 h of Q-SUN irradiation; (**c**) PP films covered with ZnT1 coating after 48 h of UV-B irradiation.

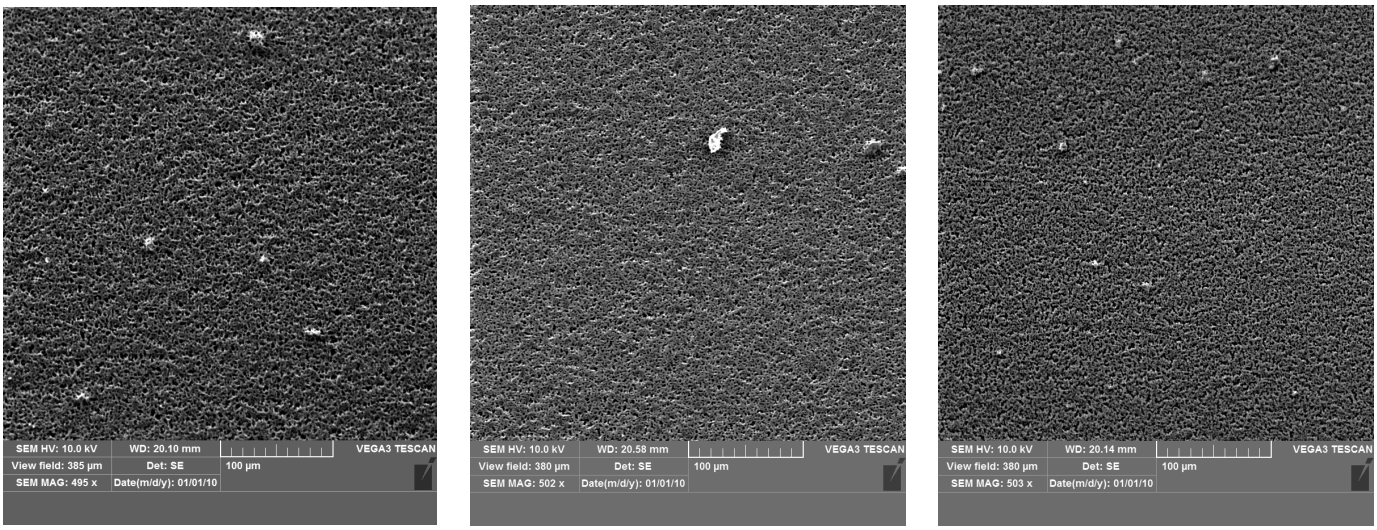

(**a**) (**b**) (**c**)

Figure 11. (**a**) PP films covered with ZnT2 coating before irradiation; (**b**) PP films covered with ZnT2 coating after 48 h of Q-SUN irradiation; (**c**) PP films covered with ZnT2 coating after 48 h of UV-B irradiation.

SEM tests showed that the uncovered PP film had a slightly rough surface (Figure 8a). The Q-SUN and UV-B irradiation had no influence on the morphology of the uncovered PP film (Figure 8b,c). As shown in Figures 9a, 10a, 11a and 12a, active coatings (Zn, ZnT1, ZnT2 and ZnT3) were clearly visible on the PP surface. In addition, it was observed that the PP film was thoroughly and homogenously covered with antiviral coatings (coated PP film samples micrographs did not reflect uncovered film samples). Additionally, UV-B and Q-SUN irradiation had no influence on the morphology of the active coatings, even moderately (Figures 9b,c, 10b,c, 11b,c and 12b,c). Observation revealed that the active covering was visible when compared to the active coatings after their accelerated irradiation (for 24 h and for 48 h). If small pores and breaks are noted on the Zn, ZnT1,

ZnT2 or ZnT3 layer, which was irradiated for 24 h or 48 h (with Q-SUN or UV-B), it would have an impact on the release of active agents from the active layers. However, small holes, pores and breaks were not observed, even after 48 h of Q-SUN and UV-B irradiation. Additionally, as can be seen in Figures 9–12, convex, spherical particles were seen on the active coatings, which may be surface contaminations.

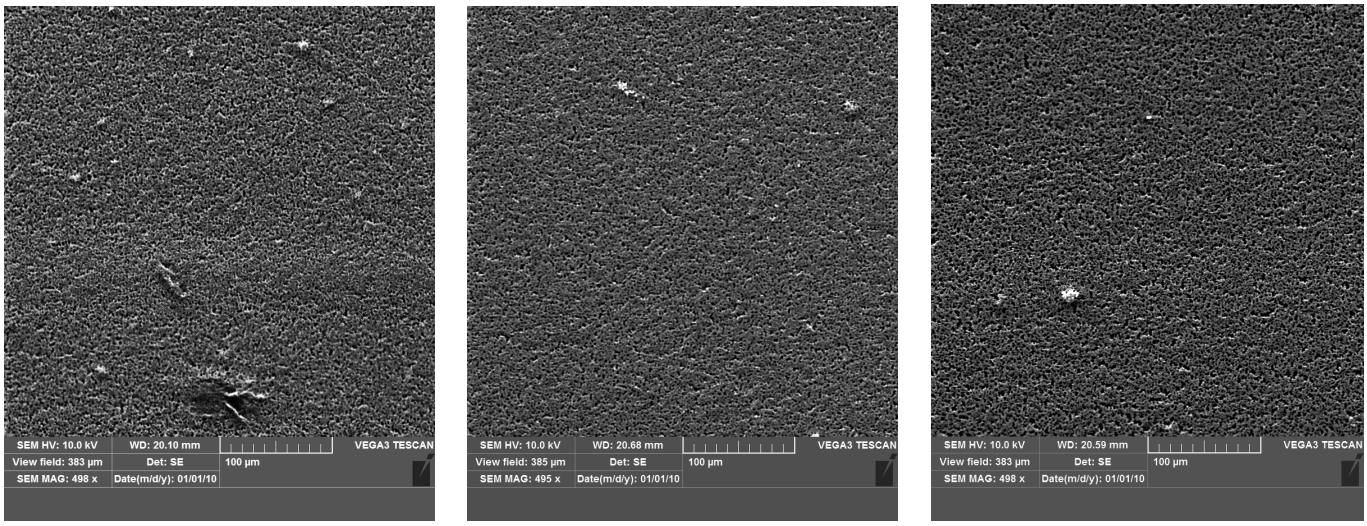

(**a**) (**b**) (**c**)

Figure 12. (**a**) PP films covered with ZnT3 coating before irradiation; (**b**) PP films covered with ZnT3 coating after 48 h of Q-SUN irradiation; (**c**) PP films covered with ZnT3 coating after 48 h of UV-B irradiation.

3.2.2. *P. syringae* Count Visualization

An experiment to test bioreactor lysis was performed, and SEM micrographs were created to view bacterial counts and fitness. The host was *P. syringae* with the phi6 phage after incubation with an active (ZnT3), non-irradiated coating, being chosen for assay to validate the antiviral properties of the layer. Additionally, the hosts with the phi6 phage after incubation with the non-coated PP film and ZnT1 (non-active) coating were used as control samples. In the case of the non-covered PP film, the results of our work indicated that *P. syringae* cells were not seen on the surface of the copper grids (Figure 13). This means that the phi6 bacteriophage was active, and it inhibited the growth of bacterial cells. The findings confirmed that the PP film had no influence on the activity of phage particles (Figure 13). Similar results were observed for the ZnT1 coating (Figure 14). A lack of bacteria on the copper grid confirmed that the layer also did not influence phage activity. Comparing the PP film and ZnT1 coating, when the phi6 phage (after its incubation with the ZnT3 layer) with the host was used (Figure 15), the incubation of this lysate with bacterial cells did not visibly influence the strain. *P. syringae* cells were visible on the surface of the copper grid, confirming good adhesion of the bacteria to the carrier. This meant that the phi6 was not active, as it had been deactivated by the ZnT3 coating.

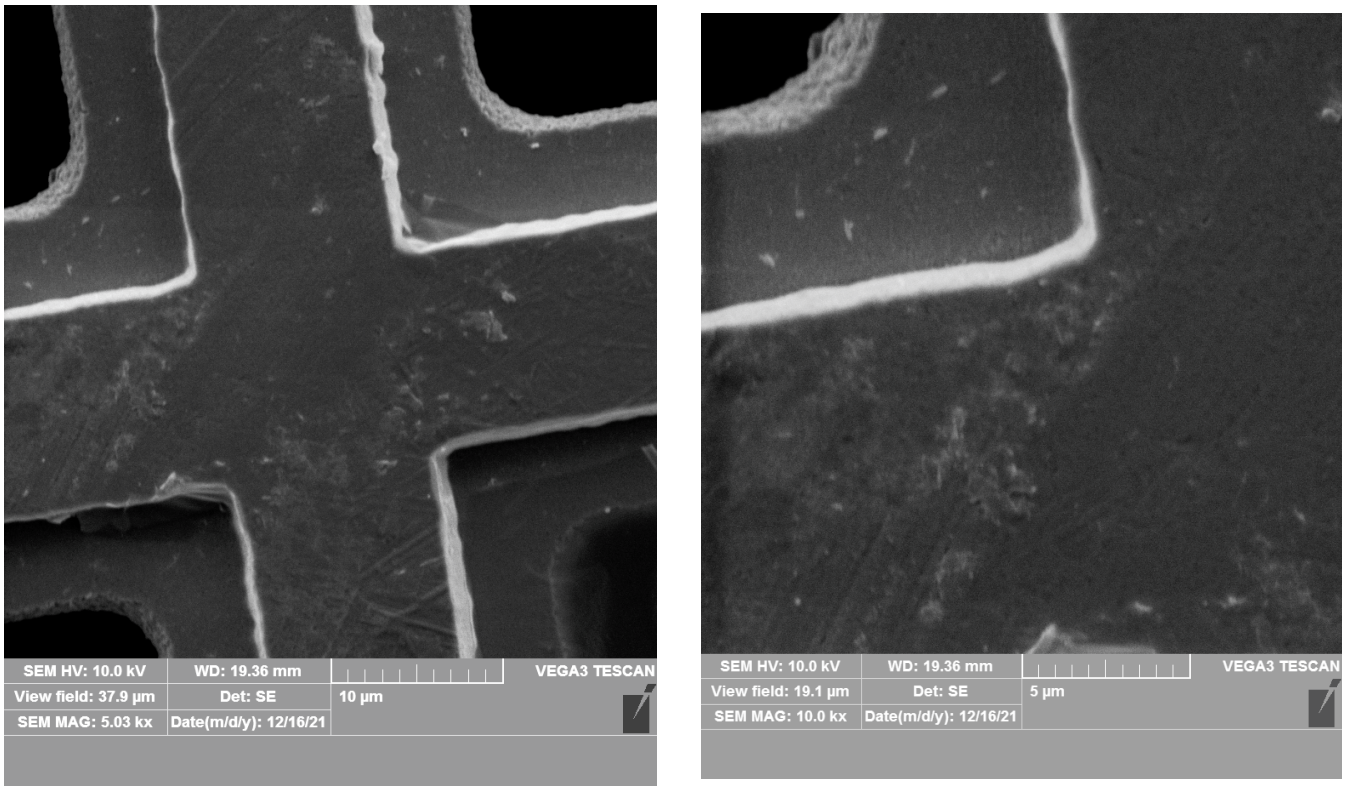

Figure 13. *P. syringe* culture after its incubation with phi 6 phages after their incubation with the PP films.

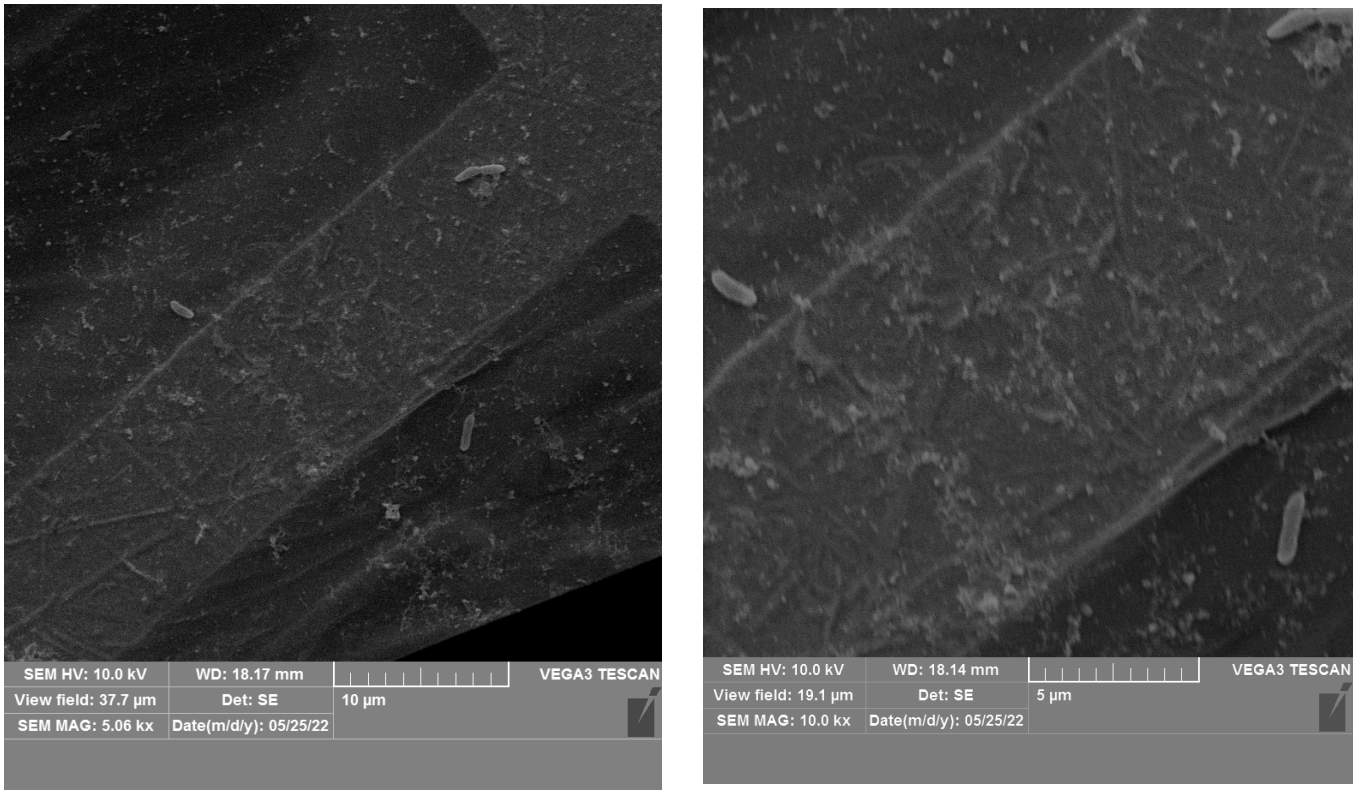

Figure 14. *P. syringe* culture after its incubation with phi 6 phages after their incubation with ZnT1 (coating containing ZnO nanoparticles and TiO_2 in the ratio: 1:1) coating.

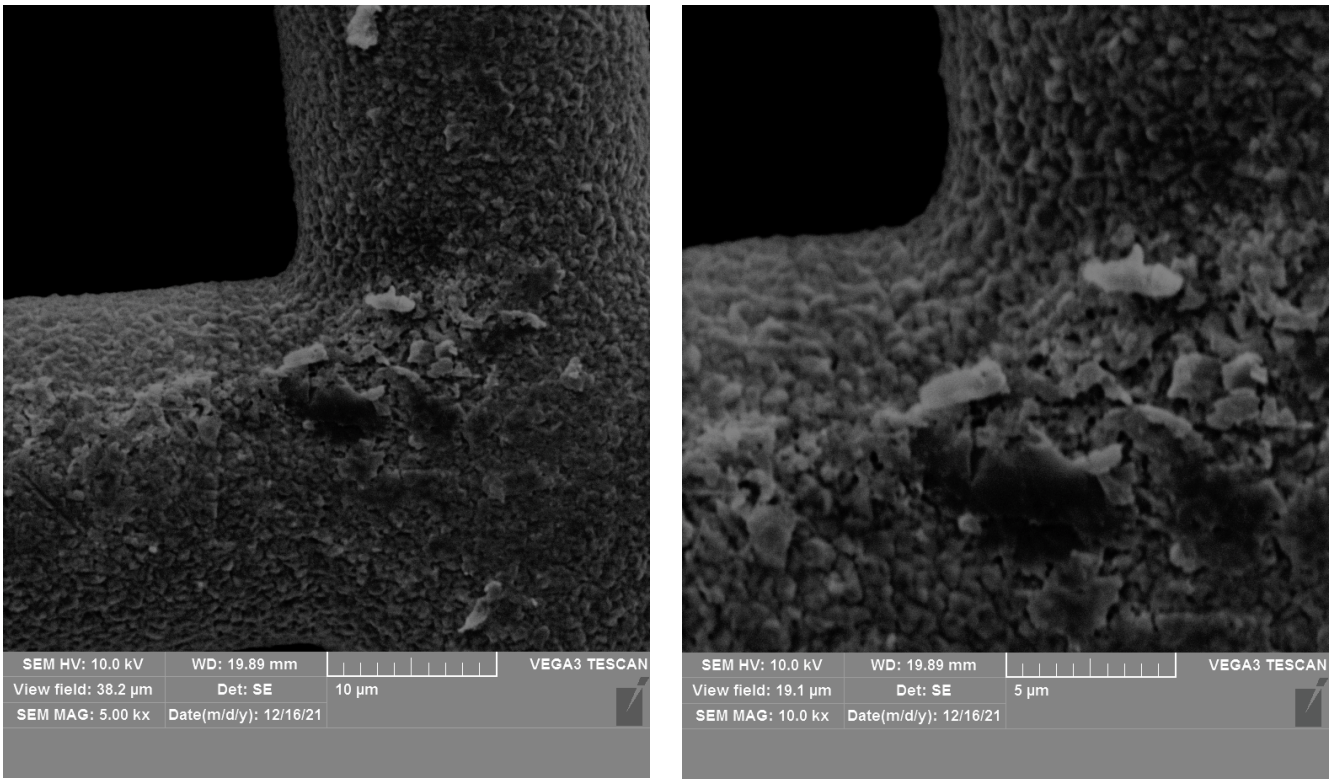

Figure 15. *P. syringe* culture after its incubation with phi 6 phages after their incubation with the ZnT3 (coating containing ZnO nanoparticles and TiO_2 in the ratio: 1:2) coating.

3.3. FTIR Analysis

The influence of Q-SUN irradiation and UV-B irradiation on active coatings may be seen through the use of FTIR spectroscopy. Analyzing the spectra of PP films (Figure 16), it was observed that there were two main regions viewed in the FTIR spectroscopy that extended through (1) ranges from 3000 to 2800 cm^{-1} and (2) ranges from 1500 to 1300 cm^{-1}. In the case of the 2951, 2915 and 2867 cm^{-1} peaks, a peak with absorption might be observed, stimulated by C-H stretch, asymmetric single bonds. Moreover, spectra peaks at 1451, 1367 and 971 cm^{-1} can be seen in a peak with CH_3-CH_2-induced absorption. Figure 16 shows the spectrum characteristic for polypropylene, which was confirmed by Prabowo et al. [33]. The results of the study showed that differences in the chemical composition and morphology of PP films (PP) after UV-B irradiation and Q-SUN irradiation were not observed. The results clearly showed that 24 h and 48 h accelerated irradiation had no influence on non-covered PP film samples (Figure 16).

The influence of 24 h and 48 h UV-B irradiation and Q-SUN irradiation on the Zn and ZnT1 active layers was also not noted. Zn Q-SUN and UV-B-irradiated coating (ZnQ24, ZnUVB24 and ZnQ48, ZnUVB48) and Q-SUN and UV-B-irradiated ZnT1 coatings (ZnT1Q24, ZnT1UVB24 and ZnT1Q48, ZnT1UVB48) are presented in Figures 17 and 18. There are four regions viewed in the FTIR spectroscopy, extending between the following: (1) ranges from 3000 to 2800 cm^{-1}; (2) ranges from 1800 to 1600 cm^{-1}; (3) ranges from 1600 to 1200 cm^{-1}; and (4) ranges from 1100 to 800 cm^{-1}. In the case of the 2919 and 2926 cm^{-1} peaks, peak consistency with absorption can be observed, stimulated by C-H stretch, asymmetric single bonds. Alternatively, spectra peaks at 1732, 1728, 1651 and 1646 cm^{-1} can be seen in a peaks stimulated by C=C stretch, double bonds. Different peak properties were shown, ranging from 1600 cm^{-1} to 1200 cm^{-1}. Further, 1452 and 1473 cm^{-1} peaks (the presence of these peaks corresponded to C-C stretch, single bonds), 1371, 1351, 1277 and 837 cm^{-1} (stimulated by C-H single bonds), and 1073, 1062, 1009 and 1006 cm^{-1} (stimulated by C-N stretch, single bonds) were observed in the case of the Zn and ZnT1

coatings before and after 24 h and 48 h of irradiation. The presence of the 1062, 1073 and 1452 cm^{-1} peaks showed that active coatings contained ZnO nanoparticles, as confirmed by Kalpana et al. [34] and Mahalakshmi et al. [35]. The presence of the 1646, 1452 and 1163 cm^{-1} peaks was found to correspond to TiO_2 presence in the Zn and ZnT1 active layers. These findings were confirmed by other authors [36–38].

The findings demonstrated that accelerated 24 h and 48 h Q-SUN or UV-B irradiation did not alter the chemical composition of the Zn and ZnT1 layers. It is tempting to suggest that the nano ZnO shielded the Zn and ZnT1 active layers against accelerated irradiation.

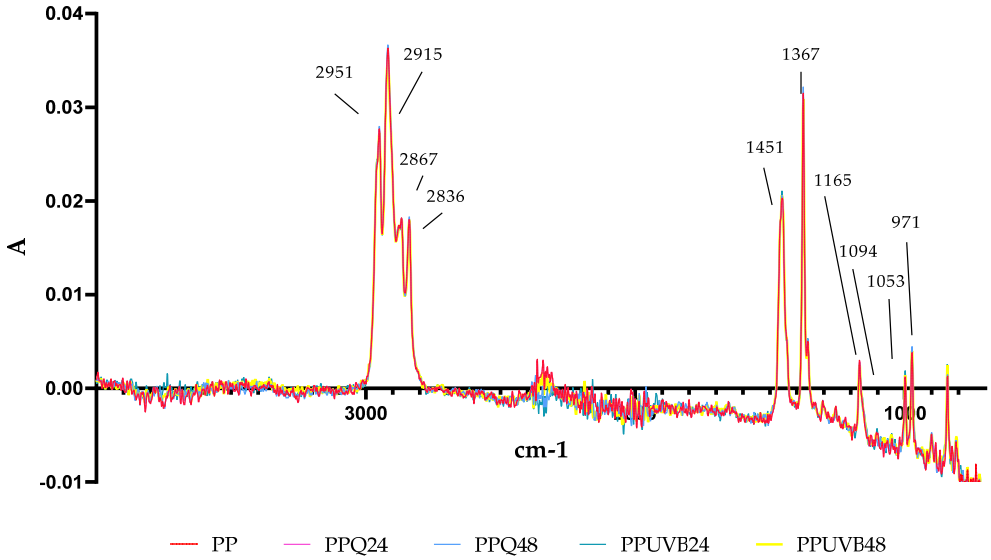

Figure 16. The FT-IR spectra of PP film coating before and after Q-SUN and UV-B irradiation (for 24 h and 38 h).

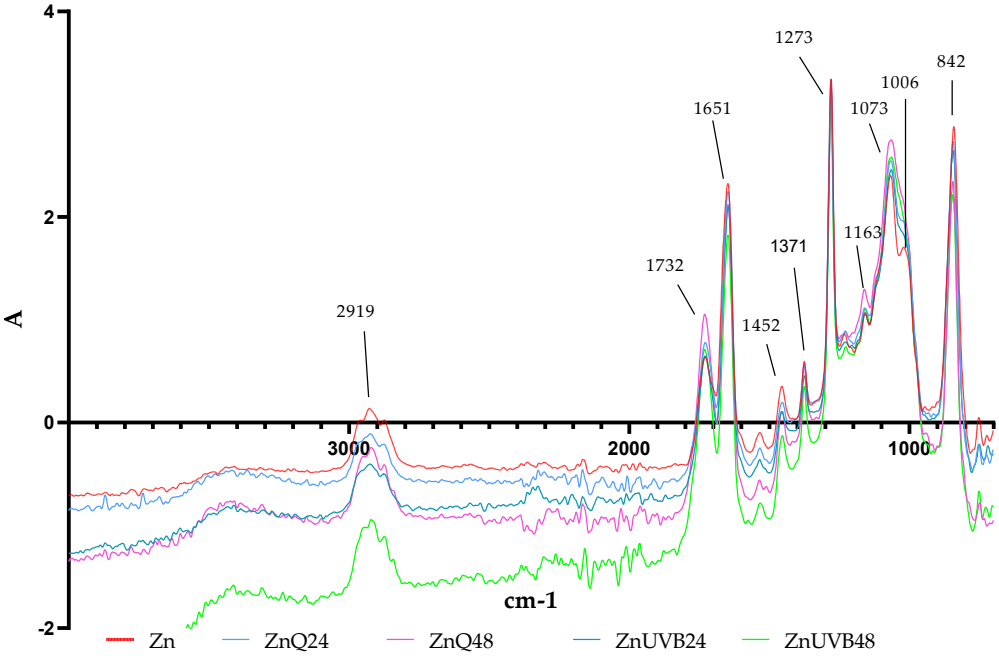

Figure 17. The FT-IR spectra of PP film covered with Zn coating before and after Q-SUN and UV-B irradiation (for 24 h and 38 h).

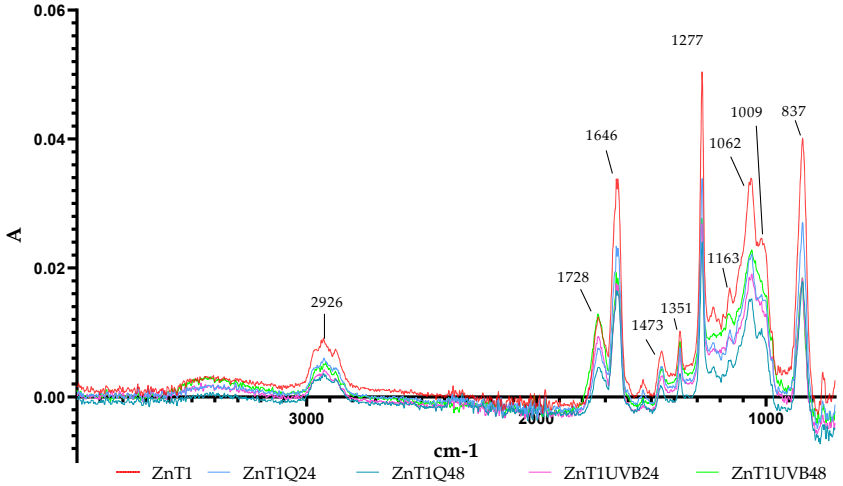

Figure 18. The FT-IR spectra of PP film covered with ZnT1 coating before and after Q-SUN and UV-B irradiation (for 24 h and 38 h).

ZnT2, a UV-B and Q-SUN-irradiated coating (ZnT2Q24, ZnT2UVB24 and ZnT2Q48, ZnT2UVB48), a Q-SUN and UV-B-irradiated ZnT3 coating (ZnT2 UVB 24 and ZnT2 UVB 48), and a UV-B-irradiated ZnT3 coating (ZnT3 UVB 24 and ZnT3 UVB 48) are presented in Figures 19 and 20. There were four regions viewed in the FTIR's spectra that extended between the following: (1) ranges from 3000 to 2800 cm^{-1}; (2) ranges from 1800 to 1600 cm^{-1}; (3) ranges from 1600 to 1200 cm^{-1}; and (4) ranges from 1100 to 800 cm^{-1}. As seen in Figures 19 and 20, for the 2915 and 2936 cm^{-1} peaks, peaks with absorption could be observed, corresponding to C-H asymmetric, stretch single bonds. On the other hand, spectra peaks at 1731, 1725, 1651 and 1650 could be observed in peaks stimulated by C=C stretch double bonds. Other peaks were noted, ranging from 1600 cm^{-1} to 1200 cm^{-1}. Further, 1453 and 1442 cm^{-1} peaks (stimulated by C-C stretch, single bonds), 1376, 1367, 1281, 843 and 842 cm^{-1} (corresponding to C-H single bonds), and 1068, 1065 and 1019 cm^{-1} (corresponded to C-N stretch, single bonds) were seen in the case of the ZnT2 and ZnT3 active layers, before and after 24 h of irradiation. The presence of the 1068, 1065 and 1442 cm^{-1} peaks determined that antiviral coatings contained nano ZnO, as confirmed by the other authors [34,35]. On the other hand, the presence of the 1650, 1651, 1442, 1453, 1160 and 1167 cm^{-1} peaks corresponded to TiO_2 presence in the ZnT2 and ZnT3 active coatings. These results were confirmed by other authors [36–38].

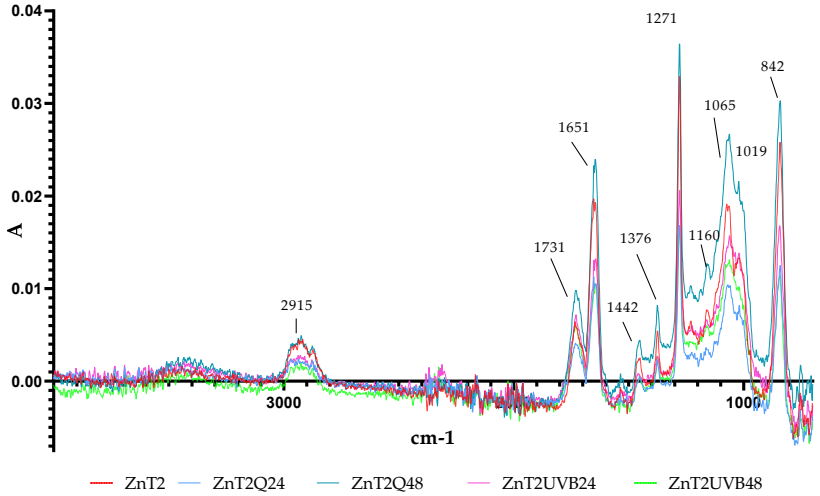

Figure 19. The FT-IR spectra of PP film covered with ZnT2 coating before and after Q-SUN and UV-B irradiation (for 24 h and 38 h).

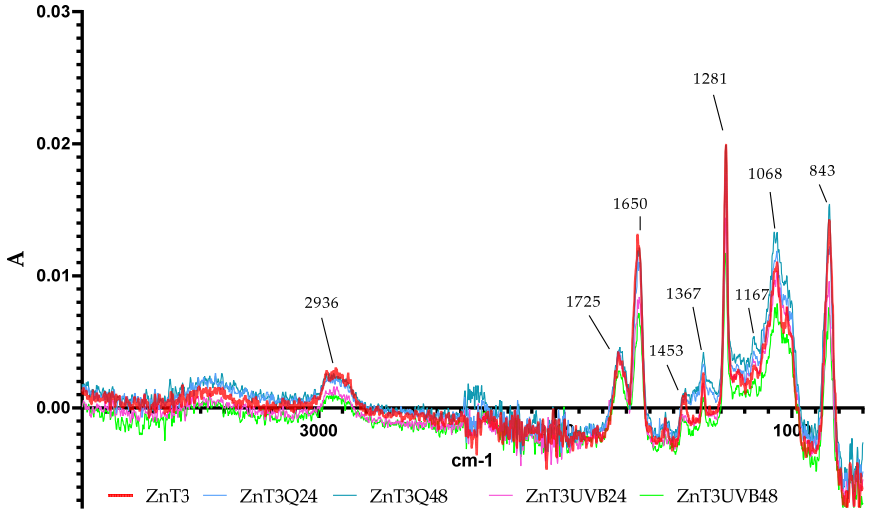

Figure 20. The FT-IR spectra of PP film covered with ZnT3 coating before and after Q-SUN and UV-B irradiation (for 24 h and 38 h).

It was clearly shown that accelerated 24 h and 48 h Q-SUN or UV-B irradiation did not influence the chemical composition of the ZnT2 and ZnT3 coatings. It was assumed that the nanoparticles of ZnO shielded the ZnT2 and ZnT3 antiviral coatings against UV-B and Q-SUN irradiation. This conclusion was confirmed by Mizielińska et al. [27,39], who used ZnO nanoparticles as an additive for an active coating created for food packaging on polyethylene films to protect them against UV irradiation. However, 24 h Q-SUN and UV-B irradiation made the coatings active against the Φ6 phage (without altering the chemical composition of the coatings). The irradiation might have activate reactive oxygen species (ROSs) production, which could inactivate bacteriophage particles.

4. Discussion

Beginning in 2019, the whole planet faced a medical emergency with the arrival of a novel, highly contagious, deadly strain, known as SARS-CoV-2 [15]. Safety concerns led to worldwide attempts to limit COVID-19 spread through hand-to-hand contact. Coating surfaces and packaging materials could be the solution [6,7]. In order to overcome the inherent shortcomings associated with the low activity of natural antiviral compounds or their sensitivity to UV aging, effective nanoparticle-based agents have been added to the coating carriers to obtain layers/covers that would function or even work actively on UV irradiation [13,15,17–19]. Many authors confirmed that both ZnO nanoparticles and TiO_2 demonstrated antiviral activity [11,15,17–19]. These findings indicated that coating materials containing ZnO nanoparticles could actively react against the phi6 phage. A previous study [6] showed that the addition of geraniol or of carvacrol into the coating carriers containing nanoparticles influenced their antiviral effectiveness, which confirmed synergy between these active compounds. Therefore, it was assumed that the addition of TiO_2 into the varnish with nano ZnO might significantly increase the activity of the coatings against the phi 6 bacteriophage. Mirzapoor et al. [13] designed and synthesized an antimicrobial layer based on $Se/TiO_2/ZnO/Ag$ nanostructures to enhance the antimicrobial activity of coating synergistically. However, our results suggest that the coatings containing ZnO nanoparticles with TiO_2 at ratios 1:1 or 1:1.5 had no antiviral activity. These findings were confirmed by SEM analysis that showed that phi6 phage particles were still active after the incubation of these coatings and inhibited bacterial cell (host) growth. Contradictory results were observed for the coating (ZnT3) containing ZnO nanoparticles and increased amount of TiO_2 (up to 1:2), which demonstrated high antiviral activity, confirming the synergistic effect between these two oxides. Additionally, SEM micrographs also revealed *P. syringae* cells, which were immobilized on the surface of the copper grid, proving that bacteriophages were inactivated by the coating. Similarly,

Zheng et al. [14] confirmed the synergistic effect between two different nanoparticles. The authors prepared Cu-TiO_2 nanofibers, which exhibited high removal efficiency in the case of bacteriophage f2 under visible light, proving the antiviral properties. The coating ZnT3 was also incubated with the phi 6 phage lysate under a visible-light tool. Wang et al. [40] designed and prepared nanomaterial based on TiO_2, showing that TiO_2 supported by single-atom nanozyme containing atomically dispersed Ag atoms (Ag-TiO_2 SAN) served as a highly efficient antiviral material that exhibited higher adsorption (99.65%) of SARS-CoV2 pseudovirus than TiO_2, which was not supported by the nanozyme. Conversely, Amiri et al. [41] confirmed that a Ag-doped TiO_2 nanocomposite demonstrated high antimicrobial properties. Similarly, Liu et al. [42] suggested that TiO_2 coating with nanostructural surface can be improved through UV irradiation.

According to Zheng et al. [14], TiO_2 may be activated by lights in the near-UV region. Mirzapoor et al. [13] suggested that when sunlight shines on the active layer containing nanoparticles, such as ZnO or/and TiO_2, the molecules of water and oxygen, along with the energy of the sun's rays, produce active compounds called VOCs and ROCs. Due to their high strength and energy, these agents may create cavities in the bacterial cell wall or virus envelopes that cause them to be destroyed. According to these suggestions, it was assumed that active coatings based on TiO_2 and ZnO nanoparticles could be activated through UV irradiation. Our results show that coatings that contained nano ZnO or ZnO nanoparticles and TiO_2 nanoparticles at a ratio of 1:1 or 1:1.5 after 24 h irradiation using the Q-SUN Xenon Test Chamber demonstrated moderate antiviral activity, meaning that Q-SUN irradiation increased their effectiveness through the activation of the nanoparticles. It was assumed that ZnO and TiO_2 in the active layer, along with the energy of Q-SUN irradiation, could produce active compounds, such as VOCs or ROCs, which might have created cavities/holes in the Φ 6 phage lipid envelope, inactivating the virus particles. It may be mentioned that FTIR analysis demonstrated that 24 h Q-SUN and UV-B irradiation did not alter the chemical composition of active coatings, which means that ZnO nanoparticles and TiO_2 were responsible for antiviral activity. Additionally, SEM analysis of the active layers demonstrated that PP films were thoroughly and homogenously covered with antiviral coatings and that the accelerated irradiation had no influence on the coatings' surface morphology. The small breaks and holes, which might release the active agents, were not visible on the surface of the active coatings. It also led to the suggestion that 24 h irradiation activated reactive oxygen species production, and these compounds could not be seen on SEM micrographs. An increase in irradiation time up to 48 h decreased the antiviral properties of the Zn, ZnT1 and ZnT2 coatings, although the coatings were still active. The ZnT3 layer containing ZnO nanoparticles and TiO_2 nanoparticles at a ratio of 1:2 (increased level of TiO_2) demonstrated high antiviral effectiveness towards the phi6 phage. Q-SUN irradiation of the coating for 24 h did not influence its activity, while longer irradiation times (48 h) had a negative effect on its properties. These results led to the conclusion that active coatings based on ZnO and TiO_2 nanoparticles (depending on the amount of TiO_2) could be activated by Q-SUN irradiation but for periods of time no longer than 24 h.

Analyzing the influence of one-day UV-B irradiation on layers and their antiviral properties, it should be mentioned that the Zn, ZnT2 and ZnT3 coatings showed moderate antiviral activity, confirming that UV-B irradiation activated the nanoparticles. It is worth mentioning that the longer UV-B irradiation (48 h) deteriorated the antiviral effectiveness of all analyzed coatings, clearly showing that UV-B irradiation should not exceed 24 h. Alebrahim et al. [2] also analyzed antiviral coatings containing TiO_2, Cu_2O, TiO_2-Cu_2O and TiO_2-Al_2O_3 nanoparticles. They confirmed that TiO_2-Cu_2O and TiO_2-Al_2O_3-based coatings had higher activity than coatings with TiO_2 and Cu_2O. As confirmed by the authors, the antiviral activity of the coatings appeared to be comparable or slightly enhanced under UVA light compared to simple ambient light. This could lead to the suggestion that UVA irradiation improved the antiviral properties of active coatings. To evaluate the ability of our coatings to offer antiviral properties, HCoV-229E coronavirus (the common cold) was trialed as a surrogate for SARS-CoV-2 by these authors [2]. Many authors have

demonstrated that bacteriophages may be used as model surrogates to replicate eukaryotic viruses. The authors used phage lysates for the development of a model to assess how viruses may be distributed with airborne particles [6,7,28]. Prussin II, A.J [28] submitted the phi6 phage as a surrogate for COVID-19. This is the reason the phage was selected as SARS-CoV-2 surrogate in the experiments in this study and in our previous work [6]. To summarize, it seems clear that the healthcare sector should develop antiviral coatings on packaging materials (as an external layer) or on surfaces against fomite transmission, which could limit super-spreading events, as in the case of SARS-CoV-2 particles and other pathogens.

5. Conclusions

The aim of the experiments in this research was to analyze the coating effectiveness of antiviral agents based on gloss varnish containing ZnO and TiO_2 nanoparticles. The novelty of this work was to investigate the influence of accelerated UV-B and Q-SUN irradiation on their effectiveness (antiviral activity of the coatings). Comparing ZnO and TiO_2 nanoparticles as photoactive metal oxides, it is worth mentioning that both ZnO and TiO_2 are excellent semiconductors, which were found to be effective against viruses, such as SARS-CoV-2. Additionally, ZnO nanoparticles were confirmed to have additional shielding properties. On the other hand, UV irradiation may not only activate materials containing these nanoparticles but can also lead to accelerated UV aging. This is why irradiation time was considered as a vitally important parameter to research. The results of our analysis determined that only one in four of the selected coatings containing nanoparticles were highly active against the phi6 phage. It should be reiterated that Q-SUN irradiation had a positive influence on the antiviral activity of the other three coatings. After 24 h of irradiation, the coatings containing lower amounts of TiO_2 than the one coating, which was found to eliminate bacteriophage particles, were noted to have moderate antiviral effectiveness, confirming that Q-SUN irradiation improved the properties of the active layers. Unfortunately, 48 h irradiation decreased the activity of the coatings, which confirmed that irradiation time should not be extended too long. Comparing the influence of the UV-B irradiation on the coating activity to the Q-SUN irradiation, it should be noted that 24 h of UV-B irradiation also improved the antiviral properties of the three coatings that were not active before irradiation. However, this decreased the activity of the coating that was shown to be active without UV-B or Q-SUN activation. Unfortunately, none of the analyzed coatings were active after 48 h of UV-B irradiation, confirming that irradiation time has to be shorter. This antiviral analysis was carried out using the phi6 phage, also known as the SARS-CoV-2 surrogate, so it could be suggested that all the coatings, which were confirmed as active against the phi6 phage, could also be effective against COVID-19 particles.

Author Contributions: M.M. and A.B. conceived and designed the experiments; M.M. wrote the paper; M.M. performed antiviral activity tests; M.M. prepared active coatings; M.M. performed SEM analysis; M.M. and A.B. analyzed the data; M.M. prepared reagents/materials; A.B. contributed analysis tools; A.B. performed statistical analysis. All authors have read and agreed to the published version of the manuscript.

Funding: This research received no external funding.

Institutional Review Board Statement: Not applicable.

Informed Consent Statement: Not applicable.

Data Availability Statement: Data are contained within the article.

Conflicts of Interest: The authors declare no conflicts of interest.

References

1. El-Fakharany, E.M.; El-Gendi, H.; El-Maradny, Y.A.; Abu-Serie, M.M.; Abdel-Wahhab, K.G.; Shabana, M.E.; Ashry, M. Inhibitory effect of lactoferrin-coated zinc nanoparticles on SARS-CoV-2 replication and entry along with improvement of lung fibrosis induced in adult male albino rats. *Int. J. Biol. Macromol.* **2023**, *245*, 125552. [CrossRef]
2. Alebrahim, E.; Khatibnezhad, H.; Bajgiran, M.M.; Solomon, M.; Liang, C.; Sagan, S.M.; Lima, R.S.; Oberste Berghaus, J.; Aghasibeig, M.; Moreau, C. A Comparative Study of the Antiviral Properties of Thermally Sprayed Coatings against Human Coronavirus HCoV-229E. *Catalysts* **2023**, *13*, 1141. [CrossRef]
3. Wolfgruber, S.; Rieger, J.; Cardozo, O.; Punz, B.; Himly, M.; Stingl, A.; Farias, P.M.A.; Abuja, P.M.; Zatloukal, K. Antiviral Activity of Zinc Oxide Nanoparticles against SARS-CoV-2. *Int. J. Mol. Sci.* **2023**, *24*, 8425. [CrossRef] [PubMed]
4. Losada-Garcia, N.; Vazquez-Calvo, A.; Alcami, A.; Palomo, J.M. Preparation of Highly Stable and Cost-Efficient Antiviral Materials for Reducing Infections and Avoiding the Transmission of Viruses such as SARS-CoV-2. *ACS Appl. Mater. Interfaces* **2023**, *15*, 22580. [CrossRef] [PubMed]
5. Mizielińska, M.; Kowalska, U.; Jarosz, M.; Sumińska, P.; Landercy, N.; Duquesne, E. The Effect of UV Aging on Antimicrobial and Mechanical Properties of PLA Films with Incorporated Zinc Oxide Nanoparticles. *Int. J. Environ. Res. Public Health* **2018**, *15*, 794. [CrossRef]
6. Mizielińska, M.; Nawrotek, P.; Stachurska, X.; Ordon, M.; Bartkowiak, A. Packaging Covered with Antiviral and Antibacterial Coatings Based on ZnO Nanoparticles Supplemented with Geraniol and Carvacrol. *Int. J. Mol. Sci.* **2021**, *22*, 1717. [CrossRef]
7. Mizielińska, M.; Bartkowiak, A. Innovations in food packaging materials. In *Food Preservation and Packaging-Recent Process and Technological Advancements*; Tumuluru, Y.S., Ed.; IntechOpen: London, UK, 2022. [CrossRef]
8. Dizaj, S.M.; Lotfipour, F.; Barzegar-Jalali, M.; Zarrintan, M.H.; Adibkia, K. Antimicrobial activity of the metals and metal oxide nanoparticles. *Mat. Sci. Eng.* **2014**, *44*, 278–284. [CrossRef] [PubMed]
9. Liu, Y.; Chen, C.; Liang, T.; Wang, Y.; Zhao, R.; Li, G.; Bai, C.; Wu, Y.; Yu, F.; Sheng, L.; et al. In vitro long-term antibacterial performance and mechanism of Zn-doped micro-arc oxidation coatings. *Colloids Surf. B Biointerfaces* **2024**, *233*, 113634. [CrossRef]
10. Oprea, A.E.; Pandel, L.M.; Dumitrescu, A.M.; Andronescu, E.; Grumezescu, V.; Chifiriuc, M.C.; Mogoantă, L.; Bălşeanu, T.-A.; Mogoşanu, G.D.; Socol, G.; et al. Bioactive ZnO Coatings Deposited by MAPLE—An Appropriate Strategy to Produce Efficient Anti-Biofilm Surfaces. *Molecules* **2016**, *21*, 220. [CrossRef]
11. Zhou, J.; Hu, Z.; Zabihi, F.; Zhu, M. Progress and Perspective of Antiviral Protective Material. *Adv. Fiber Mater.* **2020**, *2*, 123. [CrossRef]
12. Sun, Z.; Liao, T.; Sheng, L.; Kim, J.H.; Dou, S.X.; Bell, J. Fly compound-eye inspired inorganic nanostructures with extraordinary visible-light responses. *Mater. Today Chem.* **2016**, *1–2*, 84–89. [CrossRef]
13. Mirzapoor, A.; Ghashghaee, E. Nano engineered synthesis layer by layer and transparent synergistic antimicrobial coating based on Se/Ag/TiO_2/ZnO hybrid nanostructures. *Inorg. Chem. Commun.* **2023**, *153*, 110840. [CrossRef]
14. Zheng, X.; Shen, Z.; Cheng, C.; Shi, L.; Cheng, R.; Yuan, D. Photocatalytic disinfection performance in virus and virus/bacteria system by Cu-TiO_2 nanofibers under visible light. *Environ. Pollut.* **2018**, *237*, 452–459. [CrossRef] [PubMed]
15. Soni, V.; Khosla, A.; Singh, P.; Nguyen, V.-H.; Van Le, Q.; Selvasembian, R.; Hussain, C.M.; Thakur, S.; Raizada, P. Current perspective in metal oxide based photocatalysts for virus disinfection: A review. *J. Environ. Manag.* **2022**, *308*, 114617. [CrossRef]
16. Zhang, W.; Zhang, X. Adsorption of MS2 on oxide nanoparticles affects chlorine disinfection and solar inactivation. *Water Res.* **2015**, *69*, 59–67. [CrossRef]
17. Habibi-Yangjeh, A.; Asadzadeh-Khaneghah, S.; Feizpoor, S.; Rouhi, A. Review on heterogeneous photocatalytic disinfection of waterborne, airborne, and foodborne viruses: Can we win against pathogenic viruses? *J. Colloid Interface Sci.* **2020**, *580*, 503–514. [CrossRef]
18. Ditta, I.B.; Steele, A.; Liptrot, C.; Tobin, J.; Tyler, H.; Yates, H.M.; Sheel, D.W.; Foster, H.A. Photocatalytic antimicrobial activity of thin surface films of TiO_2, CuO and TiO_2/CuO dual layers on Escherichia coli and bacteriophage T4. *Appl. Microbiol. Biotechnol.* **2008**, *79*, 127–133. [CrossRef]
19. Zhang, C.; Li, Y.; Shuai, D.; Shen, Y.; Wang, D. Progress and challenges in photocatalytic disinfection of waterborne viruses: A review to fill current knowledge gaps. *Chem. Eng. J.* **2019**, *355*, 399–415. [CrossRef]
20. Kumar, S.G.; Devi, L.G. Review on modified TiO_2 photocatalysis under UV/ visible light: Selected results and related mechanisms on interfacial charge Carrier transfer dynamics. *J. Phys. Chem.* **2011**, *115*, 13211. [CrossRef]
21. Pelaez, M.; Nolan, N.T.; Pillai, S.C.; Seery, M.K.; Falaras, P.; Kontos, A.G.; Dunlop, P.S.; Hamilton, J.W.; Byrne, J.A.; O'Shea, K. A review on the visible light active titanium dioxide photocatalysts for environmental applications. *Appl. Catal. B. Environ.* **2012**, *125*, 331. [CrossRef]
22. Khraisheh, M.; Wu, L.; Ala, A.H.; Al-Ghouti, M.A. Photocatalytic disinfection of Escherichia coli using TiO_2 P25 and Cu-doped TiO_2. *J. Ind. Eng. Chem.* **2015**, *28*, 369–376. [CrossRef]
23. Liu, L.; Liu, Z.; Bai, H.; Sun, D.D. Concurrent filtration and solar photocatalytic disinfection/degradation using high-performance Ag/TiO_2 nanofiber membrane. *Water Res.* **2012**, *46*, 1101–1112. [CrossRef]
24. Liu, N.; Chen, X.; Zhang, J.; Schwank, J.W. A review on TiO_2-based nanotubes synthesized via hydrothermal method: Formation mechanism, structure modification, and photocatalytic applications. *Catal. Today* **2014**, *225*, 34–51. [CrossRef]
25. Espitia, P.J.P.; de Soares, N.F.F.; dos Coimbra, J.S.R.; de Andrade, N.J.; Cruz, R.S.; Medeiros, E.A.A. Zinc Oxide Nanoparticles: Synthesis, Antimicrobial Activity and Food Packaging Applications. *Food Bioprocess Technol.* **2012**, *5*, 1447–1464. [CrossRef]

26. Sirelkhatim, A.; Mahmud, S.; Seeni, A.; Kaus, N.H.M.; Ann, L.C.; Bakhori, S.K.M.; Hasan, H.; Mohamad, D. Review on Zinc Oxide Nanoparticles: Antibacterial Activity and Toxicity Mechanism. *Nano Micro Lett.* **2015**, *7*, 219–242. [CrossRef]
27. Mizielińska, M.; Łopusiewicz, Ł.; Mężyńska, M.; Bartkowiak, A. The Influence of Accelerated UV-A and Q-SUN Irradiation on the Antimicrobial Properties of Coatings Containing ZnO Nanoparticles. *Molecules* **2017**, *22*, 1556. [CrossRef]
28. Prussin, A.J., II; Schwake, D.O.; Lin, K.; Gallagher, D.L.; Buttling, L.; Marr, L.C. Survival of the Enveloped Virus Phi6 in Droplets as a Function of Relative Humidity, Absolute Humidity and Temperature. *Appl. Environ. Microbiol.* **2018**, *84*, 00551-18. [CrossRef]
29. Bhetwal, A.; Maharjan, A.; Shakya, S.; Satyal, D.; Ghimire, S.; Khanal, P.R.; Parajuli, N.P. Isolation of Potential Phages against Multidrug-Resistant Bacterial Isolates: Promising Agents in the Rivers of Kathmandu, Nepal. *BioMed Res. Int.* **2017**, *2017*, 3723254. [CrossRef]
30. Bonilla, N.; Rojas, M.J.; Cruz, G.N.F.; Hung, S.H.; Rohwer, F.; Barr, J.J. Phage on tap–a quick and efficient protocol for the preparation of bacteriophage laboratory stocks. *PeerJ* **2016**, *4*, 2261. [CrossRef]
31. *EN 2180-01*; ASTM Standard Test Method for Determining the Activity of Incorporated Antimicrobial Agent(s) in Polymeric or Hydrophobic Materials. ASTM: West Conshohocken, PA, USA, 2007.
32. Skaradzińska, A.; Ochocka, M.; Śliwka, P.; Kuźmińska-Bajora, M.; Skaradziński, G.; Friese, A.; Roschanski, N.; Murugaiyan, J.; Roesler, U. Bacteriophage amplification–A comparison of selected methods. *J. Virol. Methods* **2020**, *282*, 113856. [CrossRef]
33. Prabowo, I.; Pratama, J.N.; Chalid, M. The effect of modified ijuk fibers to crystallinity of polypropylene composite. *IOP Conf. Ser.: Mater. Sci. Eng.* **2017**, *223*, 012020. [CrossRef]
34. Kalpana, V.N.; Kataru, B.A.S.; Sravani, N.; Vigneshwari, T.; Panneerselvam, A.; Rajeswari, D.V. Biosynthesis of zinc oxide nanoparticles using culture filtrates of Aspergillus niger: Antimicrobial textiles and dye degradation studies. *OpenNano* **2018**, *3*, 48–55. [CrossRef]
35. Mahalakshmi, M.; Hema, N.; Vijaya, P.P. In Vitro Biocompatibility and Antimicrobial activities of Zinc Oxide Nanoparticles (ZnO NPs) Prepared by Chemical and Green Synthetic Route—A Comparative Study. *BioNanoScience* **2020**, *10*, 112–121. [CrossRef]
36. Al-Amin, M.; Dey, C.S.; Rashid, T.U.; Ashaduzzaman, M.; Shamsuddin, S.M. Solar Assisted Photocatalytic Degradation of Reactive Azo Dyes in Presence of Anatase Titanium Dioxide. *Int. J. Latest Res. Eng. Technol.* **2016**, *2*, 14–21.
37. Rajakumar, G.; Rahuman, A.A.; Roopan, S.M.; Khanna, V.G.; Elango, G.; Kamaraj, C.; Zahir, A.A.; Velayutham, K. Fungus-mediated biosynthesis and characterization of TiO_2 nanoparticles and their activity against pathogenic bacteria. *Spectrochim. Acta Part A Mol. Biomol. Spectrosc.* **2012**, *91*, 23–29. [CrossRef]
38. Chougala1, L.S.; Yatnatti1, M.S.; Linganagoudar, R.K.; Kamble, R.R.; Kadadevarmath, J.S. A Simple Approach on Synthesis of TiO_2 Nanoparticles and its Application in dye Sensitized Solar Cells. *J. Nano Electron. Phys.* **2017**, *9*, 4005-1. [CrossRef]
39. Mizielińska, M.; Kowalska, U.; Salachna, P.; Łopusiewicz, Ł.; Jarosz, M. The Influence of Accelerated UV-A and Q-SUN Irradiation on the Antibacterial Properties of Hydrophobic Coatings Containing *Eucomis comosa* Extract. *Polymers* **2018**, *10*, 421. [CrossRef]
40. Wang, D.; Zhang, B.; Ding, H.; Liu, D.; Xiang, J.; Gao, X.J.; Chen, X.; Li, Z.; Yang, L.; Duan, H.; et al. TiO_2 supported single Ag atoms nanozyme for elimination of SARS-CoV2. *Nano Today* **2021**, *40*, 101243. [CrossRef]
41. Amiri, M.R.; Alavi, M.; Taran, M.; Kahrizi, D. Antibacterial, antifungal, antiviral, and photocatalytic activities of TiO_2 nanoparticles, nanocomposites, and bio-nanocomposites: Recent advances and challenges. *J. Public Health Res.* **2022**, *11*, 4151. [CrossRef]
42. Liu, X.; Zhao, X.; Li, B.; Cao, C.; Dong, Y.; Ding, C.; Chu, P.K. UV-irradiation-induced bioactivity on TiO_2 coatings with nanostructural surface. *Acta Biomater.* **2008**, *4*, 544–552. [CrossRef]